


Review

Plasma Electrolytic Oxidation (PEO) as a Promising Technology for the Development of High-Performance Coatings on Cast Al-Si Alloys: A Review

Patricia Fernández-López ^{1,2}, Sofia A. Alves ¹, Jose T. San-Jose ² , Eva Gutierrez-Berasategui ¹ and Raquel Bayón ^{1,*}

¹ TEKNIKER, Basque Research and Technology Alliance (BRTA), Plasma Coating Technologies Unit, C/Iñaki Goenaga 5, 20600 Eibar, Spain; patricia.fernandez@tekniker.es (P.F.-L.); sofia.alves@tekniker.es (S.A.A.); eva.gutierrez@tekniker.es (E.G.-B.)

² Department of Engineering in Mining, Metallurgy and Science of Materials, Faculty of Engineering in Bilbao, Building I, University of the Basque Country (UPV/EHU), Plaza Ingeniero Torres Quevedo 1, 48013 Bilbao, Spain

* Correspondence: raquel.bayon@tekniker.es

Abstract: Cast Al-Si alloys, recognized for their excellent mechanical properties, constitute one of the most widely employed non-ferrous substrates in several sectors, and are particularly relevant in the transport industry. Nevertheless, these alloys also display inherent limitations that significantly restrict their use in several applications. Among these limitations, their low hardness, low wear resistance, or limited anti-corrosion properties, which are often not enough when the component is subjected to more severe environments, are particularly relevant. In this context, surface modification and the development of coatings are essential for the application of cast Al-Si alloys. This review focuses on the development of coatings to overcome the complexities associated with improving the performance of cast Al-Si alloys. Against this background, plasma electrolytic oxidation (PEO), an advanced electrochemical treatment that has revolutionized the surface modification of several metallic alloys in recent years, emerges as a promising approach. Despite the growing recognition of PEO technology, the achievement of high-performance coatings on cast Al-Si is still a challenge nowadays, for which reason this review aims to provide an overview of the PEO treatment applied to these alloys. In particular, the impact of the electrolyte chemical composition on the properties of the coatings obtained on different alloys exposed to harsh environments has been analyzed and discussed. By addressing the existing gaps and challenges, this paper contributes to a better understanding of the intricacies associated with the development of robust PEO coatings on cast Al-Si alloys.

Keywords: plasma electrolytic oxidation (PEO); cast Al-Si alloys; coatings; lightweighting



Citation: Fernández-López, P.; Alves, S.A.; San-Jose, J.T.; Gutierrez-Berasategui, E.; Bayón, R. Plasma Electrolytic Oxidation (PEO) as a Promising Technology for the Development of High-Performance Coatings on Cast Al-Si Alloys: A Review. *Coatings* **2024**, *14*, 217. <https://doi.org/10.3390/coatings14020217>

Academic Editor: Jinyang Xu

Received: 28 December 2023

Revised: 4 February 2024

Accepted: 7 February 2024

Published: 9 February 2024



Copyright: © 2024 by the authors. Licensee MDPI, Basel, Switzerland. This article is an open access article distributed under the terms and conditions of the Creative Commons Attribution (CC BY) license (<https://creativecommons.org/licenses/by/4.0/>).

1. Introduction

Aluminum (Al) is frequently alloyed with various elements to produce a diverse range of commercial alloys. Among these, cast aluminum–silicon (Al-Si) alloys stand out, constituting over 80% of the globally produced cast Al alloys [1,2]. These alloys offer interesting advantages, including excellent castability and weldability, a high strength-to-weight ratio, optimal melt fluidity, and cost-effective manufacturing [2–4]. The alloying of cast Al-Si alloys involves elements such as Si, Cu, Mg, Zn, Ni, or Fe, among others. The specific properties of these alloys are determined by their chemical composition. Si serves as the principal alloying element of cast Al-Si alloys, typically ranging between 4% and 24% [5]. These alloys are classified as hypoeutectic (Si wt.% < 11), eutectic (Si wt.% ~11), and hypereutectic (Si wt.% > 11) based on their Si content [1,6]. During the manufacturing of castings, the inclusion of Si requires longer solidification times, favoring a higher fluidity and lower shrinkage, and enhancing castability and weldability [1,3,6]. Furthermore, the addition of Si reduces the melting point of the resulting alloy, which is beneficial for the

industrial casting processes [7]. Cu and Mg are other commonly added alloying elements in cast Al-Si alloys. The addition of Cu, typically ranging from 1% to 5%, improves the hardening of the alloy in both the as-cast condition and during heat treatments [5,6]. On the other hand, Mg is usually added in lower quantities (usually 0.2%–0.6%) [5] and serves as a precipitation hardener, improving both the tensile properties at high temperatures (up to 200 °C) and enhancing creep resistance [1,6]. Other alloying elements, such as Ni or Zn, are usually incorporated to enhance the tensile strength or to improve the properties after heat treatment without compromising ductility, respectively.

In cast Al-Si alloys, Fe typically emerges as the predominant undesirable impurity [1,8], with its concentration being higher in recycled alloys, where it can elevate to approximately 1% [9]. Due to the limited solubility of Si and Fe in the Al matrix, brittle intermetallic compounds, such as $\text{Al}_{15}(\text{FeMn})_3\text{Si}_2$ or $\text{Al}_{15}(\text{FeMnCr})_3\text{Si}_2$, can be formed (Figure 1) [4,10], often resulting in a degradation of the mechanical properties of the alloy [9]. Nevertheless, in the manufacturing of cast Al-Si alloys using specific techniques like high-pressure die-casting (HPDC), the presence of Fe could be advantageous due to its role in preventing molten alloys from adhering to the casting matrix [8] and reducing adhesion [11]. HPDC, renowned for its cost-effectiveness and capability to manufacture components with complex geometry and thin walls, stands as the predominant method for the manufacturing of cast Al-Si components [12,13]. Nonetheless, the turbulences generated by the high-speeds applied result in both superficial and internal porosities in HPDC components, which could compromise some mechanical properties [4,14].

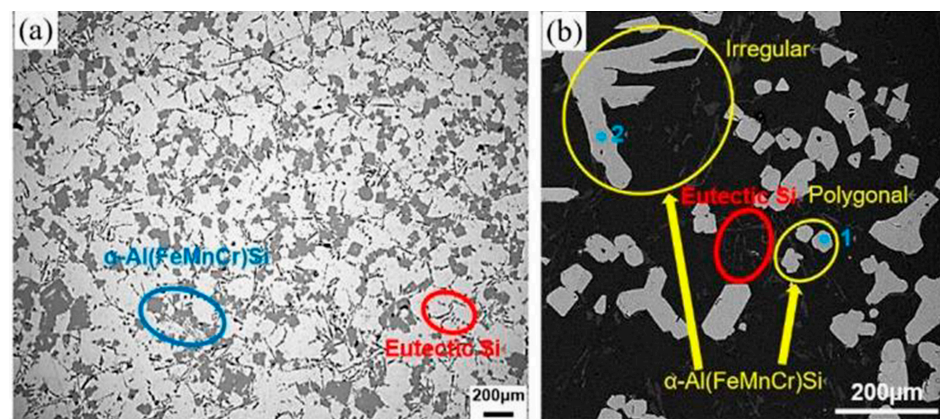


Figure 1. Optical (a) and SEM (b) micrographs of an $\text{AlSi}_7\text{FeMn}_{1.5}\text{Cr}_{0.5}$ alloy containing iron-rich intermetallic compounds [15]. Reprinted from Materials Letters; 277; Dongtao Wang, Xiaozu Zhang, Hiromi Nagaumi, Xinzhong Li, Haitao Zhang; 3D morphology and growth mechanism of cubic $\alpha\text{-Al}(\text{FeMnCr})\text{Si}$ intermetallic in an Al-Si cast alloy; 128384; Copyright (2020), with permission from Elsevier.

Due to their outstanding properties, cast Al-Si alloys are extensively used in the automotive industry [4], and their application in the aerospace industry is also growing [7,16] (Figure 2). The primary advantage of the use of cast Al-Si alloys in the transport sector resides in the lightweighting achieved in comparison with other conventional materials, like steel or cast iron [17,18], offering a substantial reduction of fuel consumption, CO_2 emissions, and overall carbon footprint [19,20]. In a mid-size vehicle, one ton of Al replacing conventional materials can lead to an 18-ton reduction in GHG emissions throughout its whole life cycle [21]. Cast Al-Si alloys serve as effective substitutes for cast iron or steel in several automotive components, including those with complex geometries, like engine blocks or cylinder heads [20,22], cylinder liners [23], and pistons [1]; power train applications [18]; brake parts [24]; wheels [25]; and larger structural components [26].



Figure 2. Schematic representation of components manufactured from cast aluminum alloys.

Despite the promising features offered by cast Al-Si alloys, their industrial implementation faces significant limitations, especially in applications that require prolonged durability under aggressive environments. Their poor tribological features, including low wear and abrasion resistances [4,16,27], low hardness, and high tendency to adhesion [28,29], constitute the primary drawbacks. Concerning corrosion resistance, although Al alloys generally provide acceptable corrosion resistance due to their natural oxide layer, this protection is often inadequate under harsh environments, particularly for cast Al-Si alloys, due to the relevant heterogeneities in their chemical composition. Furthermore, the high Si content promotes localized corrosion, rendering them unsuitable for applications with severe requirements compared to wrought Al alloys [4,16,30–32].

Surface engineering, which emerged in the 1970s, entails the modification of coating material surfaces and serves as a powerful tool, not only for the enhancement of the materials, but also to provide them with novel functionalities. Reinforcement, modification, functionalization, or embellishment are among the technological and functional demands faced by materials across several industrial sectors. Addressing these requirements, alongside considerations such as sustainability and durability, constitutes critical elements in the design and advancement of the latest generation of surface solutions to overcome the most demanding challenges imposed by strategic industrial sectors.

Anodic oxidation, commonly known as anodizing, stands as a traditional and extensively used technique for enhancing the surface properties of Al alloys, particularly for the improvement of the anti-wear and anti-corrosion capabilities. During this process, an anodic oxide film is electrochemically generated on the surface of Al under anodic polarization. This involves the anodic dissolution of the metal and the subsequent reaction between the Al cations (Al^{3+}) and the negatively charged anions from the acid solution in which the treated component has been immersed, resulting in the formation of a metal oxide film [33]. Different types of anodizing are available, such as chromic acid anodizing for high protection, sulphuric anodizing for aesthetic and protective films, and hard anodizing for thicker coatings. Despite its widespread application in recent years, the current use of anodizing is facing limitations due to stringent EU policies restricting the use of acid electrolytes. Furthermore, anodizing proves inadequate for treating the surfaces of cast Al-Si alloys, particularly those with higher Si contents. This challenge is exacerbated when dealing with recycled cast Al-Si alloys containing complex intermetallic compounds. Challenges associated with the treatment of these alloys arise from silicon phases hindering the proper development of the anodic layer [16], which results in differing conductive behavior

between the Al matrix and the dispersed Si phases, leading to variations in the growth rate of the anodic oxide coating [3]. These discrepancies in the growth rates give rise to the oxide layers of reduced thickness and hardness (up to 800 HV), increased heterogeneity [4], as well as heightened porosity and brittleness [34], rendering their application unfeasible, especially in more severe environments.

The growing demand for lightweight materials within the transport sector, especially in automotive manufacturing, has prompted the exploration and refinement of advanced technologies for the surface modification of Al alloys, particularly targeting cast Al-Si alloys. Among these techniques, plasma electrolytic oxidation (PEO) has emerged as a promising method garnering significant interest for its capability to enhance the durability and corrosion resistance of these alloys. Surface treatment of cast Al-Si alloys results more complex compared to wrought Al alloys due to their complex microstructure, which presents unique challenges. The widespread usage of these alloys in the transport sector underlines the necessity for robust and effective surface engineering solutions.

This review provides a comprehensive description of the complexities associated with the PEO treatment of cast Al-Si alloys, placing its relevance in context with conventional surface modification techniques such as anodizing. A detailed examination of PEO technology delves into the coating growth mechanism and the key influencing process parameters, encompassing substrate composition, electrolyte composition, and the type of power supply used. This is succeeded by a thorough review of the pertinent literature, exploring the impact of different electrolyte formulations (silicate based, phosphate based, and aluminate based) on the development of high-performance PEO coatings for cast Al-Si substrates. Given the challenges linked with the treatment of cast Al-Si alloys, in addition to addressing considerations related to the type of electrolyte used, strategies for improving PEO coatings are addressed. This encompasses the examination of pre- and post-treatments, as well as the incorporation of nanoparticles and microparticles into the electrolyte, a promising frontier to further improve the functional attributes of PEO-treated cast Al-Si alloys. By synthesizing these insights, this review aims to offer an overview of the current state of knowledge, identify critical research gaps, and lay the basis for future advances in the search for surface modification solutions for cast Al-Si alloys in different applications within the transport sector.

2. Plasma Electrolytic Oxidation (PEO)

Plasma electrolytic oxidation (PEO), also known as microarc oxidation (MAO), represents an electrochemical plasma-assisted technology employed for the development of multifunctional ceramic coatings on diverse valve metals. PEO combines electrochemical oxidation processes with plasma discharges, thereby sintering the treated metal surface. Within the metallic substrates treated by PEO, Al [35,36], Ti [37,38], and Mg [39,40] alloys stand out, while nowadays the technology is also being extended to other metallic substrates, like Zr [41], Nb [42], Ta [43], and even steel [44–46].

The properties of the PEO coatings are strongly related to the type of alloy treated [4,47], the chemical composition of the electrolyte used [4,23,48], and the electrical parameters applied during the process [49–51]. Notable properties of PEO coatings include high wear resistance [4,23,52], strong corrosion protection [53,54], high hardness [55,56], and excellent adhesion to the metallic substrate [57]. The morphology of PEO coatings is also suitable for the adhesion of other top coats, like sol–gel layers, while it could act as a reservoir for liquid or solid lubricants, providing self-lubricating properties [58–60]. Furthermore, PEO coatings exhibit high thermal resistance [61,62], superior dielectric properties [63,64], or photo-catalytic features [38,65,66]. In the biomedical industry, PEO coatings provide desirable properties such as biocompatibility [67,68], antibacterial properties [67,69], and bioactivity [70,71].

Discharge phenomena that occurred during electrolysis were initially observed by Sluginov around the year 1880 [72]. However, the technologies related to this phenomenon and their applications gained more attention during the 20th century. Researchers such

as Snezhko et al. [73], Markov et al. [74,75], Kurze et al. [76,77], and Yerokhin et al. [78] significantly contributed to the understanding of these technologies. During this period, various terms have been employed to describe PEO technology, including micro-plasma oxidation, anode spark electrolysis, or plasma electrolytic anode treatment [79].

The PEO process constitutes an electrochemical procedure wherein the treated sample or component is immersed in an electrolytic bath [80,81], while an electric current and a potential are applied. This process requires two electrodes: the treated sample, serving as the anode and connected to the positive output of the power supply; and a cathode enveloping the treated sample [80,82], usually made of stainless steel [83–85] and connected to the negative output of the power supply [80] (Figure 3a).

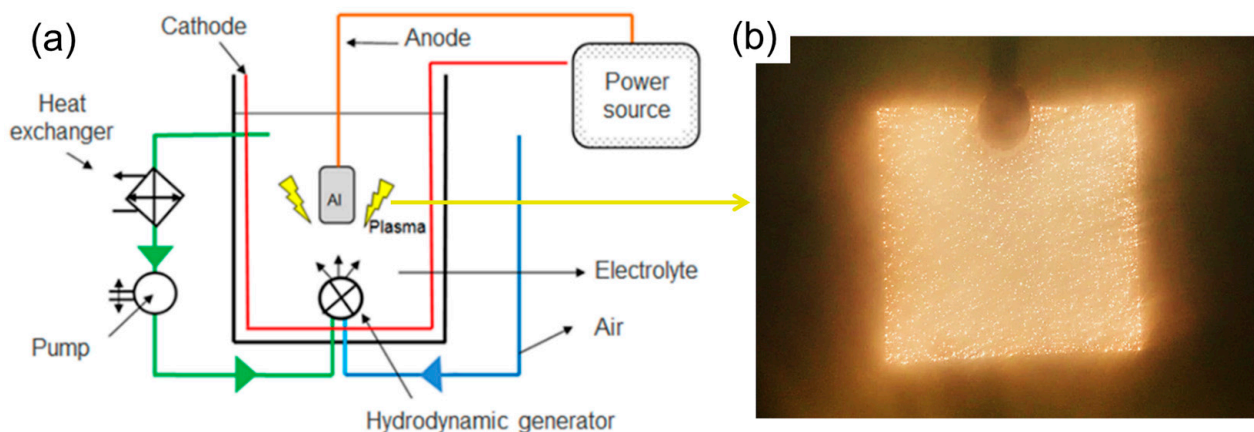


Figure 3. (a) Schematic representation of the PEO equipment and (b) plasma micro-discharges occurring during a PEO process on an Al sample carried out at Tekniker.

During a PEO process, the treated sample undergoes anodic polarization to high voltages, typically ranging from 300 V to 700 V, exceeding the dielectric breakdown voltage threshold of the pre-existing oxide layer [86–88]. During the treatment, there is also a continuous release of gas in the form of gas bubbles surrounding the anode. The establishment of a high electric field between the anode and the cathode results in the ionization of these gas bubbles, leading to the generation of plasma micro-discharges (Figure 3b) characterized by high temperatures, around 1500 °C, resulting in localized melting of the metal substrate. As a result, multiple and complex electrochemical reactions take place simultaneously, involving specific reactions with ions from the electrolyte, mainly oxygen. These plasma-chemical reactions culminate in the formation of the coating oxides, which solidify instantaneously as the overall temperature of the system remains refrigerated [89,90]. Therefore, the PEO treatment requires the development of specific electrochemical processes that include anodic oxidation of the treated metallic substrate [91–93], electrolysis of water, promoting gas evolution [57,91], and thermo-chemical reactions including the deposition of electrolyte-discharged anions [93–95].

PEO technology could be considered an evolution of anodizing for metal protection [16]. However, although both technologies work under a similar basic procedure, PEO involves higher potentials, reaching hundreds of volts [96], leading to more complex reactions and growth mechanisms [97]. Furthermore, compared with anodization, PEO technology results in thicker and denser coatings [98], which are also less detrimental to the fatigue limit of the alloy [99]. From an industrial perspective, PEO would be easier to apply than anodization, with less critical pre-treatment requirements and PEO can be carried out under atmospheric working environments, which would greatly simplify the whole manufacturing process [98,100]. Moreover, another outstanding advantage that makes PEO be viewed as a promising technology is the fact that employs water-based alkaline electrolytes without heavy metals, which are much less harmful to the environment than

the acidic solutions used in anodizing [88,101]. The main differences between anodizing, hard anodizing and PEO have been summarized in Table 1.

Table 1. Comparison of the processing conditions and properties obtained in anodizing, hard anodizing, and PEO treatments.

Parameter	Anodizing	Hard Anodizing	PEO
Pre-treatment	Critical		Not necessary
Electrolyte	Acidic (sulphuric, chromic, oxalic, etc.)		Alkaline without heavy metals
Potential applied	10–50 V	20–120 V	Higher than breakdown voltage
Current density	Low: $<10 \text{ A}\cdot\text{dm}^{-2}$		Medium-high: $5\text{--}25 \text{ A}\cdot\text{dm}^{-2}$
Metallic substrate	Critical	Medium	High versatility
Adhesion to the substrate	Good	Moderate	High
Time	Moderate: 10–60 min	High: 30–120 min	Low $< 10 \text{ min}^*$
Coating growth rate	Low: $<1 \mu\cdot\text{min}^{-1}$	Medium: $1\text{--}3 \mu\cdot\text{min}^{-1}$	High: $1\text{--}5 \mu\cdot\text{min}^{-1}$
Microstructure	Amorphous		Amorphous and crystalline
Energy consumes	Low	Medium	Medium-high
Eco-friendly	No	No	Yes

* For the development of coatings with thicknesses typically applied by anodising. Thicker PEO coatings will require longer treatment times.

The assessment of PEO technology in relation to other conventional surface modification methods is context dependent, with each technique offering distinct advantages and drawbacks based on factors like material properties, specific requirements, and intended use cases. Regarding the surface modification of Al alloys, it is generally accepted that PEO technology results in coatings of considerable thickness, superior substrate adhesion, and exceptional wear and corrosion resistance, all while maintaining an environmentally sustainable profile. The PEO process also offers versatility across alloys and geometries, but requires precise control of parameters and can consume more energy than other conventional techniques. Moreover, the relatively high surface roughness and scalability issues are relevant constraints that are currently limiting the industrialization of this technology.

2.1. PEO Coating Growth Mechanism

The PEO coating growth is governed by two main mechanisms: the micro-discharge mechanism and the coating growth mechanism [102]. The micro-discharge mechanism, although not fully understood, is explained by three main theories [103]. The first, referred to as local avalanche breakdown [104,105], proposes that each micro-discharge results from localized electron avalanches in the bulk of the anodic film, leading to the breakdown of the solid insulating coating. Albella et al. proposed an extension of this theory, suggesting that the electrolyte species incorporated into the coating initiate electron avalanches, leading to plasma micro-discharges [106,107]. However, the expected linear relationship between applied voltage and coating thickness does not match practical observations [108]. The second theory, usually referred to as glow discharge electrolysis, suggests that the initial breakdown of the barrier layer is induced by free electrons from the electrolyte that are injected into the gas bubbles at the oxide/electrolyte interface. This theory was defended by Wang et al. [109], who found that anions from the electrolyte, other than OH^- , minimally influenced the composition of the active plasma species. According to this theory, the glow discharges would promote the melting and sintering of the underlying ceramic coating. The third model, known as the discharge-in-pore theory, assumes that micro-discharge initiation occurs at the bottom of the micropores of the coating by gas discharge [110].

Among these, the local avalanche breakdown is the most widely accepted theory [111], suggesting that electron avalanches promoting the micro-discharges would also form

discharge channels in the oxide layer [112]. To explain the growth of a PEO coating on pure Al, Monfort et al. [113] used a silicate- and phosphate-based electrolyte and studied the distribution of the electrolyte species throughout the coating, finding that coating growth occurred at dielectric breakdown sites, creating short-circuit pathways. These pathways, enriched with phosphorus at the metal/coating interface, facilitated the penetration of species from the electrolyte into the interior of the coatings.

The development of a PEO process and the associated coating growth mechanism is typically divided into four stages [114–116] (Figure 4). During the first stage, the voltage experiences a rapid and linear increase, similar to conventional anodic oxidation, and the substrate is covered only by a thin layer of Al_2O_3 . After reaching the breakdown voltage, plasma micro-discharges gradually appear on the surface of the treated sample [25,117] (Figure 4). In the second stage, the voltage increases more slowly, promoting the growth of the PEO coating through the formation of the oxide phases. During the third stage, the potential remains at a near-stable value, indicating the transformation of the previously formed oxides into crystalline phases [118]. At this stage, the growth thickness of the coating is also almost unaffected by the total current density.

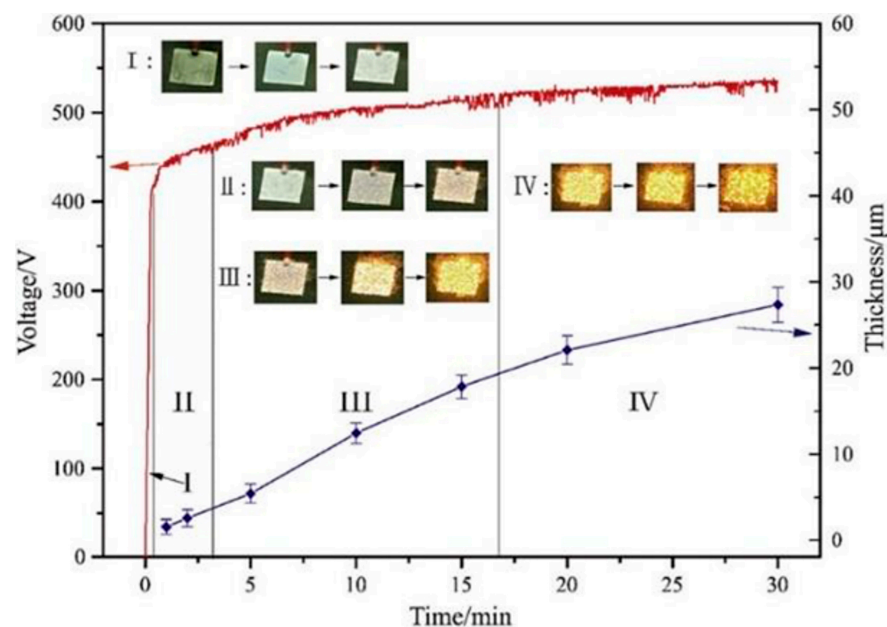


Figure 4. Typical evolution of the potential over time during a PEO process, with the corresponding plasma micro-discharges on the surface of the treated Al alloy [114]. Reprinted from Journal of Alloys and Compounds; 753; Rui-qiang Wang, Ye-kang Wu, Guo-rui Wu, Dong Chen, Dong-lei He, Dalong Li, Changhong Guo, Yefei Zhou, Dejiu Shen, Philip Nash; An investigation about the evolution of microstructure and composition difference between two interfaces of plasma electrolytic oxidation coatings on Al; 272–281; Copyright (2018), with permission from Elsevier.

In certain PEO processes, the potential evolution may not follow the typical pattern shown in Figure 4, leading to a phenomenon known as “soft sparking”. This particular regime occurs in those PEO processes where the applied cathodic current density is higher than the anodic current density, $R = J_{\text{cathodic}}/J_{\text{anodic}} > 1$, resulting in a drop in the positive potential [119], and typically leads to a refinement of the plasma micro-discharges, in terms of light and sound emissions [88,120].

Although the mechanism behind soft sparking, is not yet fully understood, it is correlated with an increased resistance to energy transfer due to the thicker and denser coating formed [121]. The earlier appearance of the soft sparking regime has also been associated with the use of aged electrolytes, due to the decrease in ionic species that reduce the electrical conductivity of the electrolyte while modifying the plasma discharges [122]. This regime would not only avoid the occurrence of aggressive plasma discharges, but

the more refined discharges associated with it would promote the development of PEO coatings with enhanced properties [57]. For example, it has been found that soft sparking promotes denser inner layers in PEO coatings developed on Al substrates, together with a higher formation of α -Al₂O₃ [119]. Furthermore, the transition to the soft sparking regime will also favor an improved energy efficiency of the process, due to the reduction of the total power consumption as a consequence of the lower potential during the process [87].

The morphological structure of PEO coatings typically shows three distinct layers. The outer layer, usually comprising between 5 and 30% of the coating thickness, usually shows defects (i.e., cracks and/or pores) and is mainly composed of γ -Al₂O₃ with relatively low hardness values, around 500 HV and 1000 HV [31,115]. The intermediate layer, which accounts for between 70 and 95% of the total coating thickness, is denser and consists of both γ -Al₂O₃ and α -Al₂O₃, with higher hardnesses ranging from 900 HV to 2000 HV [31,115,123]. Adjacent to the substrate, an amorphous Al oxide inner layer promotes strong adhesion to the coating [102,124]. Nevertheless, recent advances have reported bi-layered PEO coatings, where the outermost layer promotes higher density. This particular structure has been observed in PEO coatings developed on cast Al-Si alloys using aluminate-based electrolytes that promote a higher rate of Al₂O₃ into the coating [4,14,23]. This particular morphology would be explained by the fact that the oxidation and incorporation of the Si from the substrate promotes the formation of Si- or aluminosilicate oxides, with a lower density than the Al oxides, while the NaAlO₂ from the electrolyte promotes a higher proportion of Al₂O₃ in the outermost layer [54,125].

2.2. PEO Process Parameters

The key factors influencing the properties of PEO coatings on cast Al-Si alloys include substrate composition, electrolyte composition, and electrical process parameters such as the type of power supply or the voltage and current density applied. These factors affect the thickness, composition, and morphology of the coating and ultimately the performance of the coating in various environments. For example, variations in substrate composition can alter the adhesion and mechanical properties of PEO coatings, while the chemical composition of the electrolyte can directly influence the formation of specific oxide phases, thereby affecting the corrosion resistance and tribological properties of the developed coatings.

2.2.1. Substrate Composition

During the PEO process, part of the metallic substrate is dissolved. This actively contributes to the formation of the ceramic coating. Consequently, the chemical composition of the treated alloy plays a key role in determining the composition, microstructure, and characteristics of the resulting coating [52,126,127]. Previous investigations have shown that the presence of alloying elements, such as Cu, Mg or Zn in Al alloys, inhibits the transition of γ -Al₂O₃ to α -Al₂O₃ [102,128]. This suppression of the phase transformation is attributed to the lower bond energy between the oxygen and these alloying elements, compared to the robust interaction between Al and O₂. Under the influence of the electric field, Cu²⁺, Mg²⁺, and Zn²⁺ ions would migrate to the outer part of the coating faster than the Al²⁺ ions. The presence of these weaker bonds in the lattice would disrupt the grain growth, as the transformation from γ -Al₂O₃ to α -Al₂O₃ involves a shift from cubic to hexagonal packing, typically accompanied by grain growth and an increase in the transition temperature [127]. In the particular case of cast Al-Si alloys, the Si will also significantly inhibit the effective growth of the PEO coating [127,129].

2.2.2. Electrical Parameters

A PEO process can be carried out under direct current (DC), alternating current (AC), and unipolar pulsed (UP) or bipolar pulsed (BP) current, with the type of power supply being a determining factor in the characteristics of the PEO coating. DC, which provides the lowest energy efficiency, represents the simplest mode and its application is best suited

for treating components with a simple geometry that requires low thicknesses [130]. The AC mode improves the process control but has limitations in terms of power and current frequency. This mode provides coatings with better properties than those obtained with DC sources and also allows better control of the discharge parameters and processes. However, the control provided is sometimes insufficient for the design of PEO coatings with certain requirements [131]. According to the literature [132], the processes performed using pulsed sources show the most successful results in terms of energy efficiency.

In addition to the type of power supply, precise control of various electrical parameters is essential, including anodic and cathodic potentials, applied current density, frequency, duty cycle, process time, and temperature. Among these, the most relevant parameters to control are the current density, frequency, and anodic potential. The anodic potential is particularly relevant because it provides the energy required to form the coatings and significantly influences the microstructure and properties of the PEO coatings [102]. Once the applied anodic potential exceeds the value of the critical breakdown voltage of the barrier layer of the metal substrate, plasma micro-discharges occur on the treated sample [57]. Increasing the anodic potential leads to an increase in the number, brightness, and size of the plasma micro-discharges, as long as a limiting voltage value is not exceeded, and beyond which the above-mentioned behavior of the plasma discharges is reversed. The same pattern is observed for micropores, where higher anodic potentials lead to an increase in both size and number [133].

The applied current density, which directly determines the growth rate of the PEO coating, is primarily determined by the nature of the alloy being treated. Typically, applying too low current densities would lead to a relatively slow coating growth rate, which would impair the energy efficiency of the process. On the other hand, the use of excessive current densities will promote a PEO coating with lower mechanical properties and higher roughness, a higher release of gaseous products, and the treated sample may even be burnt [100,134]. Al alloys containing low amounts of alloying elements will typically require current densities between $5 \text{ A}\cdot\text{dm}^{-2}$ and $15 \text{ A}\cdot\text{dm}^{-2}$. However, Al alloys with higher amounts of alloying elements, and especially cast Al-Si alloys, will require current densities of around $25 \text{ A}\cdot\text{dm}^{-2}$ [4,14,23]. In terms of frequency, higher frequencies usually result in coatings with lower roughness and provide shorter plasma discharge lifetimes, reducing the occurrence of large destructive discharges [134]. The roughness of the coating is also proportional to the process time applied: longer processes will increase the arc force occurring at the surface and promote higher discharges, resulting in more uneven surfaces [134].

2.2.3. Electrolyte

The electrolyte is probably the most important parameter in a PEO process, as it determines not only the course of the process, but also the microstructure, composition, and properties of the developed coatings [135,136]. Typically, PEO electrolytes are water-based alkaline solutions, enriched with various inorganic salts, nanoparticles, or additives [100]. This makes PEO electrolytes environmentally friendly, which is a major advantage over anodizing, which employs acidic electrolytes.

The chemical composition of the electrolyte is critical because its constituents are incorporated into the PEO coating through the plasma-chemical reactions that take place during the process [37,101]. PEO electrolytes also provide oxygen, which reacts with the molten cations of the metal substrate, resulting in the formation of ceramic oxides, such as Al_2O_3 or TiO_2 for Al and Ti alloys, respectively [38]. The movement of OH^- through the electrolyte, under the influence of the electric field, favors the oxygen transport mechanism to the metallic substrate [57]. In addition, the electrolytes contain other compounds that confer anionic or cationic components to the PEO coating [38].

PEO electrolytes are typically categorized based on the predominant inorganic compound in their formulation, with common classifications including silicate-, aluminate- and phosphate-based electrolytes. Among these, silicate-based electrolytes, with Na_2SiO_3

being the most common reagent, are the most widely used electrolytes in PEO technology [64,137,138]. In general, silicate-based electrolytes have been found to be more stable than phosphate-based electrolytes [101]. However, for certain alloys and applications, such as cast Al-Si alloys with high tribological requirements, these electrolytes may not be the most appropriate. This is attributed to their tendency to promote an excessive presence of Si oxides, mullite, and aluminosilicates within the coating, which are also derived from the Si in the metal substrate. Consequently, these coatings exhibit inferior tribological properties compared to Al oxides [139]. In the case of phosphate-based electrolytes, some studies have reported their ability to enhance the density and tribological performance of the coating [140]. Furthermore, it is common for phosphorus salts to be incorporated into silicate- or aluminate-based electrolytes at lower concentrations than the latter [141,142]. Although research on aluminate-based electrolytes is comparatively recent, observations suggest that they favor the development of coatings with high tribological and anti-corrosion performance. This is particularly notable in the treatment of complex cast Al-Si alloys, where the main interest resides in increasing the Al oxides in the coating to counteract the formation of Si oxides originating from the substrate [54,128,136].

The chemical stability of the electrolyte also plays a key role, as inadequate dispersion of the reagents can lead to the formation of precipitates. This would not only hinder the reaction and incorporation of the components into the coating, but could also cause blockages in the electrochemical cell pipes. Continuous use induces aging of the electrolyte, gradually depleting its ionic species and decreasing its electrical conductivity, thereby affecting the potential breakdown value and the plasma discharge formation during the process [122]. Nevertheless, it has also been observed that electrolyte aging would favor the occurrence of soft sparking by increasing the α -Al₂O₃ content in the coating [122]. Therefore, the evaluation of the electrolyte quality must be analyzed on a case-by-case basis. The pH values of the PEO electrolytes typically range between 10 and 13, and this is usually regulated by the addition of KOH or NaOH [57,88]. However, it is critical to control the concentration of these reagents, as their higher concentration has previously been found to result in a lower coating growth rate due to an increased anodic dissolution [130,143]. The electrical conductivity of the electrolyte, which typically varies between 5 and 100 mS·cm⁻¹, is also a crucial parameter, directly influencing the breakdown value during the PEO process (higher electrical conductivity corresponds to a lower breakdown potential) [57,144]. Unlike anodizing, the temperature control during PEO processes, especially in Al alloys, is less sensitive [145]. However, for titanium alloys, the temperature of the electrolyte during the process plays a more significant role. For example, an aluminate-based electrolyte used in the PEO coating of Ti showed an increased amount of α -Al₂O₃ at lower electrolyte temperatures [146].

Structural defects such as porosity and microcracking are common despite the improved wear and corrosion resistance of PEO coatings. These defects usually result from gas release or rapid cooling during the formation of the micro-electrical discharges. Consequently, the high porosity and the presence of defects will induce the development of more brittle layers, limiting their long-term barrier efficacy. In particular, the incorporation of specific chemical elements, such as certain salts or nanoparticles, into PEO coatings is of great interest to reduce the intrinsic porosity of these layers, thereby providing coatings with a broader range of properties [147,148]. Each additive, depending on the concentration used and how it is combined with the other additives, will provide unique properties to the developed PEO coating, such as higher growth rate, higher thickness and hardness, lower roughness, or enhanced tribological and anti-corrosion performance [86,149–151].

One of the major challenges in PEO technology involves the mitigation of the intrinsic porosity of PEO coatings, which typically compromises an optimal tribological and corrosion performance. Porosity can be reduced through the use of several approaches, including the adjustment of electrical parameters, the development of duplex coatings, and the modification of the electrolyte composition. Among these methods, the formulation of the electrolyte emerges as the most effective method of porosity reduction, with emphasis

on the incorporation of micro- or nanoparticles. Generally, particles are directly introduced into the electrolyte in the form of powders or sols comprising different compounds [62]. The incorporation of the particles or nanoparticles can be accomplished through either an inert or reactive mechanism [152]. The type of incorporation will depend on the substrate, electrical process parameters, electrolyte composition, and inherent properties of the particles. In the case of an inert incorporation, no reaction nor formation of a new phase occurs. Additionally, the size and shape of the particles undergo minimal alteration after their incorporation. Conversely, in reactive incorporation, the particles react with compounds from both the electrolyte and the metal substrate. This process is more complex and influenced by several parameters [153]. The reactive incorporation is more feasible in particles with smaller sizes and relatively low melting points [153,154].

Achieving a proper and adequate dispersion of the particles in the electrolyte is critical for the optimal incorporation of the particles into the coating. When dispersion is unstable, particles tend to agglomerate, forming clusters of larger size, even micrometric. In addition, introducing pigments and/or dyes to the electrolyte can confer aesthetic functionality, leading to the generation of PEO coatings with different colors. In general, black is the most demanded color due to its aesthetical functionality and its ability to provide coatings with high emittance and absorbance, properties required in aerospace internal components subjected to significant thermal gradients in space [35,155]. However, producing black PEO coatings remains challenging, particularly on more challenging alloys like cast Al-Si alloys. Three reagents, namely potassium fluorotitanate (K_2TiF_6), sodium tungstate (Na_2WO_4), and ammonium metavanadate (NH_4VO_3), have been extensively studied for obtaining black PEO coatings. It should be noted that, unlike anodizing which uses coloring agents, the black coloring in PEO coatings can also be obtained by the reaction and dissociation of these reagents during the process, resulting in oxides with a dark grey or black color. Among the aforementioned reagents, K_2TiF_6 stands out for the dark color that it provides to the coating, increased thickness [86], enhanced wear and corrosion resistance [82,156–159], as well as heightened absorbance and emissivity values [35]. Na_2WO_4 is widely used in formulating silicate- [86,97,160–162], aluminate- [155], and phosphate-based [163,164] electrolytes, resulting in black coatings on Al [162,164] and titanium [163] substrates. Tungsten-containing electrolytes, when applied to Al substrates, typically form an $Al_2(WO_4)_3/Al_2O_3/Al$ composite [165]. The surface energy of the $Al_2(WO_4)_3$ /electrolyte interface is higher than that of the Al_2O_3 /electrolyte interface, so the tungsten-containing oxides are located in the outer part of the coating, providing a darker color. Furthermore, the addition of Na_2WO_4 improved the corrosion resistance [35,155], and catalytic properties [66,165] of the coatings.

NH_4VO_3 has also been employed for the development of black coatings [164,166], but its toxicity significantly limits its use. Besides black, PEO coatings with other colors have also been obtained, through the additivation of the electrolytes with dyes or pigments [167] (Figure 5).

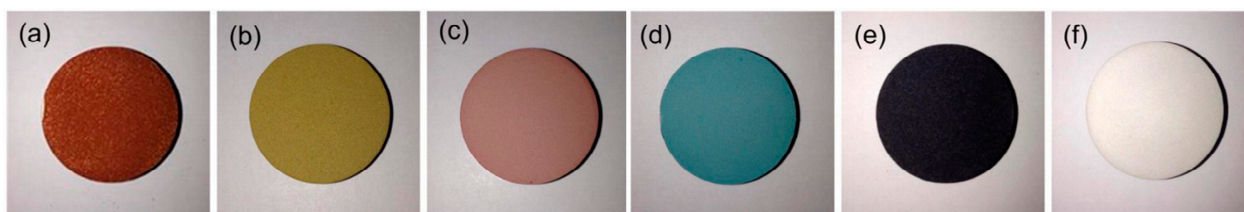


Figure 5. (a) Red, (b) yellow, (c) orange, (d) blue, (e) black, and (f) white PEO coatings obtained by adding dye emulsions to an electrolyte in an Al substrate [168]. Reprinted from Surface and Coatings Technology; 287; Shang-Chun Yeh, Dah-Shyang Tsai, Jian-Mao Wang, Chen-Chia Chou; Coloration of the aluminum alloy surface with dye emulsions while growing a plasma electrolytic oxide layer; 61–66; Copyright (2016), with permission from Elsevier.

3. Surface Modification of Cast Al-Si Alloys through PEO Technology: A Current Challenge

The development of protective coatings on cast Al-Si alloys by conventional anodizing is challenging, mainly due to the hydration of the silicon phases [34,169]. Although PEO technology has been widely used for the development of coatings on several Al alloys (2024, 6061, 7075, etc.), and has obtained high-performance coatings, the development of competitive PEO coatings on cast Al-Si alloys remains a challenge nowadays. However, despite the higher complexity of this type of alloy, there has been an increase in the number of publications in recent years, highlighting the interest and the need for the surface improvement of these alloys using PEO technology.

The chemical composition of the electrolyte used in the PEO process is a critical determinant of the microstructure, composition, and performance of the coatings. Different electrolyte formulations, such as silicate-, phosphate-, and aluminate-based solutions, offer different advantages and challenges. Selecting the electrolyte composition is therefore critical to tailoring the properties of PEO coatings to meet the specific performance requirements of cast Al-Si alloys. The published findings related to the growth of PEO coatings on different cast Al-Si alloys have been analyzed and classified according to the type of electrolyte used: silicate-, phosphate- or aluminate-based. The factors hindering the surface treatment of cast Al-Si alloys using PEO technology have been analyzed, as well as the different strategies described in the literature for the improvement of the coatings obtained.

3.1. PEO Coatings Developed on Cast Al-Si Alloys Using Silicate-Based Electrolytes

Silicate-based electrolytes are the most widely used within PEO technology. In one of the first studies carried out concerning the development of PEO on cast Al-Si alloys, Krishtal et al. [170] studied the influence of Si content on the properties of the developed PEO coating. For this aim, they treated hypoeutectic, eutectic, and hypereutectic alloys. The authors showed that the composition and microstructure of the cast Al-Si alloy directly influenced the growth of the PEO coating, determining the morphology of the PEO coating. Furthermore, the authors observed that the Si particles present in the Al matrix inhibited the reaction between Al and O₂, hindering the growth of the PEO coating due to the lower electrical conductivity of the Si phases with respect to the Al matrix. As a consequence, the layers obtained not only showed lower thickness, but also poorer hardness and adhesion, together with higher porosity [170].

In another early research project on this topic, Wang & Nie [171] studied the influence of Si content on the growth mechanism, composition, and morphology of the coating. For that purpose, they worked with a hypoeutectic (A319) and a hypereutectic (A390) alloy, using an electrolyte composed of 4 g·L⁻¹ Na₂SiO₃ [171]. The authors observed that the Si content significantly influenced the lifetime and morphology of the coating during stages I, II, and III of the PEO process. Although the breakdown voltage value was similar for the hypo- and hypereutectic alloys—390 V and 400 V, respectively—the hypoeutectic alloy reached that value in 1 min, while the hypereutectic alloy required 5 min to reach 400 V. This slower rise in potential at the beginning of the process would indicate a lower coating growth rate on the alloy with the higher Si content. This reduced coating growth would be a consequence of the lower Al area to be passivated in the hypereutectic alloy during this initial stage [171]. A similar pattern was observed in the rate of increase in the potential during stages II and III. In the second stage, the alloy A319 required 1 min to raise the positive voltage by 50 V, while the alloy A390 required 5 min to increase the voltage value up to 65 V. In the third stage, the rate of potential rise was 2.79 V·min⁻¹ and 1.65 V·min⁻¹ for alloys 319 and 390, respectively. The coatings obtained during stage IV showed a similar composition, mainly γ -Al₂O₃, and similar roughness for both alloys. In addition, the authors also determined that the alloy composition did not lead to significant variations in the coating for thicknesses above 50 microns [171].

Wang & Nie [171] also studied the variation in coating morphology throughout stages II, III, and IV for A319 and A390. In the second stage, it was observed, by means of

SEM and EDS analysis, that the plasma micro-discharges started at the interface between the Al matrix and the Si grains due to a concentration effect of the electric field in that interface. That discharge would melt the Si phase, mixing it with the Al oxide, leading to the formation of aluminosilicates (Al-O-Si), which have a lower melting point than the Al oxides, and whose morphology presented cavities and bubbles. Since the A390 alloy contained higher Si content and, therefore, higher discharge points at the Al-Si interface, it required a higher potential for the occurrence of the discharges. During stage III, due to the higher presence of Al-O-Si compounds in the coating, with a lower melting point and higher porosity, more discharge points appeared in those areas, leading to a clustering of the aluminosilicate phases. In stage IV, due to the increased thickness of the coating, the chemical reactions involved more elements from the electrolyte than from the substrate. In addition, at this stage, the morphology and composition of the coatings developed on the A319 and A390 alloys became more uniform [171].

Xue et al. [169] investigated the development of PEO coatings with high anti-corrosion performance on cast Al-Si alloys with a 7% Si content. They developed coatings with different thicknesses, comparing the morphology and chemical composition of each one, using an electrolyte composed of Na_2SiO_3 and KOH. In this study, the results concerning the coating growth and the evolution of the potential agreed with those obtained by Wang & Nie [171]. The coating growth rate increased during the second stage of the process, decreasing during the third stage. The coatings obtained in that study exhibited three distinct regions: the inner layer, which showed high adhesion to the metal substrate, an intermediate layer, with high density, and a porous outer layer (Figure 6). From the EDS analysis, it was found that the intermediate dense layer was mainly composed of Al oxides, while a significantly higher amount of Si was detected in the porous outermost layer. The porous outer layer, besides Si, also showed higher Na and K content (Figure 6).

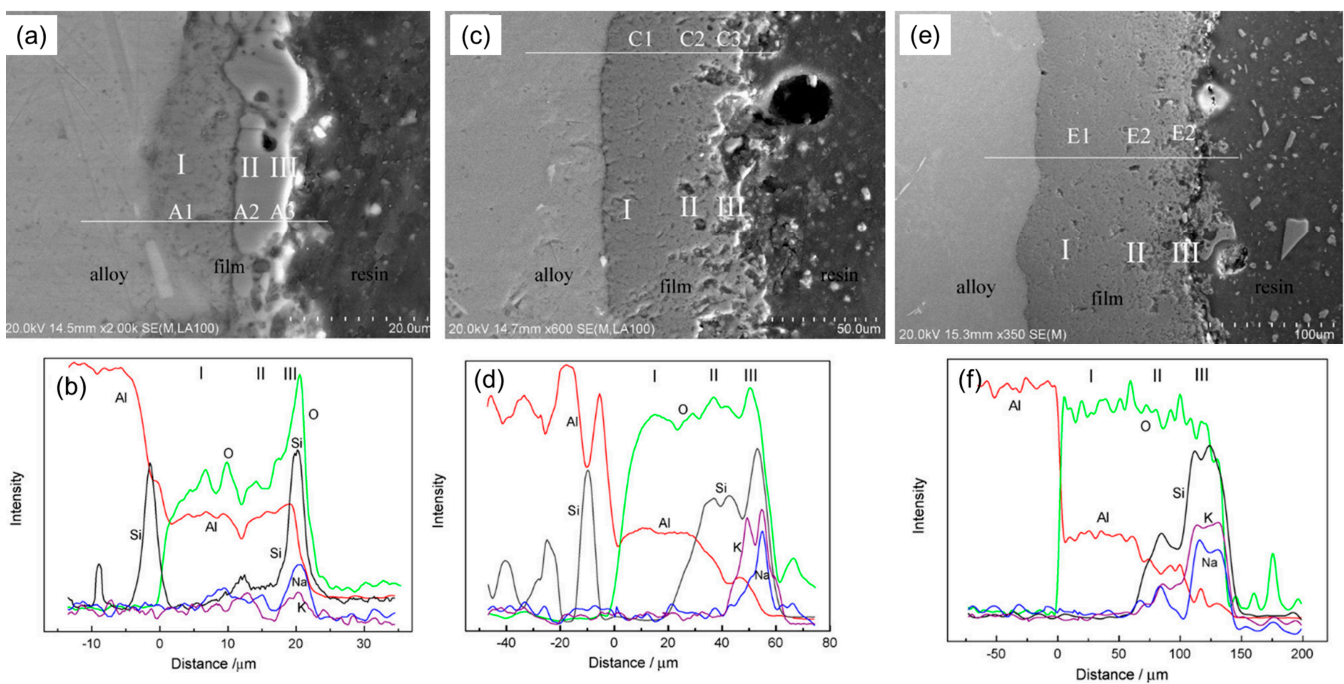


Figure 6. Cross-sections and their corresponding EDS analysis of PEO coatings developed using a silicate-based electrolyte, with thicknesses of 20 μm (a,b); 60 μm (c,d); and 140 μm (e,f) [169]. Reprinted from Applied Surface Science; 253; Wenbin Xue, Xiuling Shi, Ming Hua, Yongliang Li; Preparation of anti-corrosion films by microarc oxidation on an Al-Si alloy; 6118–6124; Copyright (2007) with permission from Elsevier.

According to the authors [169], the Si, Na, and K present in the porous outer layer would have come from the electrolyte (more specifically, Na and K were not present in the alloy, only in the electrolyte), and did not diffuse into the intermediate dense layer. Xue et al. [169] suggested that this result was mainly due to the use of an AC power supply, which favors the obtention of denser coatings on cast Al-Si alloys. The higher density of the coatings would prevent the diffusion of the ions from the electrolyte towards the innermost layers, remaining in the external zone, where the higher porosity of this region would favor their permanence. Concerning the oxide phases detected in the coatings, γ -Al₂O₃ phases were detected in all coatings, while α -Al₂O₃ was only found in the thickest coatings (60 μ m and 140 μ m). Mullite phases were also detected in all the coatings, although their content increased with increasing the coating thickness. It also investigated the influence of PEO treatment on the corrosion behavior of the cast Al-Si alloy [169]. For this purpose, they compared the corrosion resistance of the cast Al-Si reference alloy against three samples treated by PEO, with thicknesses of 20 μ m, 60 μ m, and 140 μ m. Electrochemical corrosion tests showed that both general and pitting corrosion resistance improved considerably with the application of the PEO coating. Moreover, the improvement is even more pronounced with increasing coating thickness, with the best results being obtained for the coating of 140 μ m.

The influence of Si phases on the growth, composition, and morphology of PEO coatings on cast Al-Si was also studied by He et al. [34]. In this study, cast Al-7Si alloys were treated using an electrolyte composed of Na₂SiO₃, KOH, and Na₃AlF₆, using a pulsed bipolar power supply at a frequency of 700 Hz. Based on SEM and EDS analysis, it was observed that the coating grown on the Al primary phases was mostly composed of Al₂O₃, while Si and O₂ content increased in the eutectic α phase areas, due to the relative oxidation of Si. The eutectic β phase regions showed a higher Si and O₂ content, but there was no evidence of plasma discharge in these regions. This would indicate that Si oxides could have been formed by melting and oxidation due to the high temperature of the plasma discharges in the Al substrate regions, mixing with the Al₂O₃ phases during the coating growth process. He et al. also observed that the Si content decreased from the outer to the inner region of the coating, suggesting that the higher Si content in the outer region would come from the silicate-based electrolyte. In a further step, Xu et al. [129] treated hypereutectic cast Al-Si alloys with a Si content between 27 and 32%, using an electrolyte composed of Na₂SiO₃ and NaOH, and an AC power supply. It was observed that longer PEO processes, up to 300 min, resulted in more uniform coatings, both in terms of element distribution and coating morphology.

Sabitini et al. [29] carried out research in which the main objective was the comparison of the growth, properties, and wear resistance of the PEO layers grown, under the same process conditions, on a cast A359 and a wrought 7075 alloys. The authors used a 50 Hz AC power supply and a commercial silicate-based electrolyte. Due to the higher presence of microstructural defects in the cast alloy caused by the presence of Si phases in the substrate (Figure 7), the coatings grown on this material showed lower hardness and lower elastic modulus, as well as higher roughness (Figure 8). Both PEO coatings on cast and wrought alloys showed an improvement in wear resistance compared to the base materials. At high loads, the coating developed on the 7075 wrought alloy showed a stronger tribological performance than the coating grown on the cast Al-Si alloy, due to the higher hardness and homogeneity of the former. Feng Su et al. [172] also studied the development of a PEO coating with high tribological performance on an A356 casting alloy. In this case, they employed a pulsed power supply under a frequency of 2000 Hz, and two different electrolytes, containing only K₄P₂O₇, and K₄P₂O₇ combined with Na₂SiO₃. In the tests, carried out under minimum lubrication, a tribological improvement (lower COF, wear, and plastic deformation) was found in the PEO coatings compared to a PTWA coating.

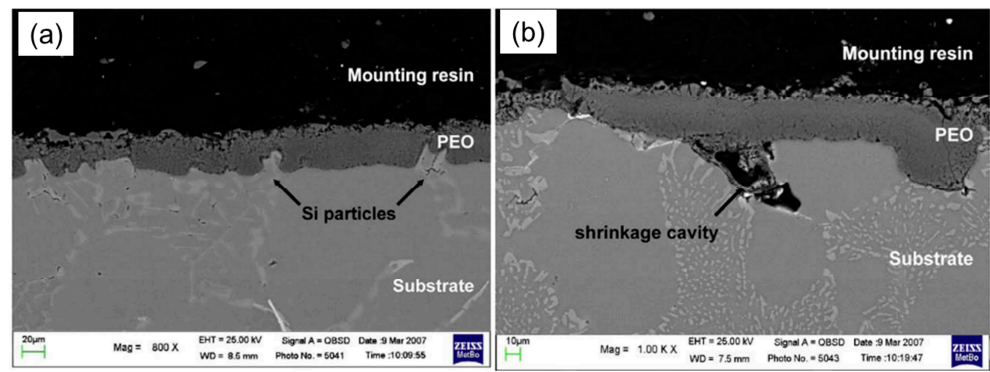


Figure 7. Cross-sectional SEM micrographs of the PEO coating developed on an A359 cast Al-Si alloy showing particular morphologies, such as eutectic Si particles (a) and shrinkage cavities (b) [29]. Reprinted from Materials & Design; 31; G. Sabatini, L. Ceschini, C. Martini, J.A. Williams, I.M. Hutchings; Improving sliding and abrasive wear behaviour of cast A356 and wrought AA7075 aluminium alloys by plasma electrolytic oxidation; 816–828; Copyright (2010), with permission from Elsevier.

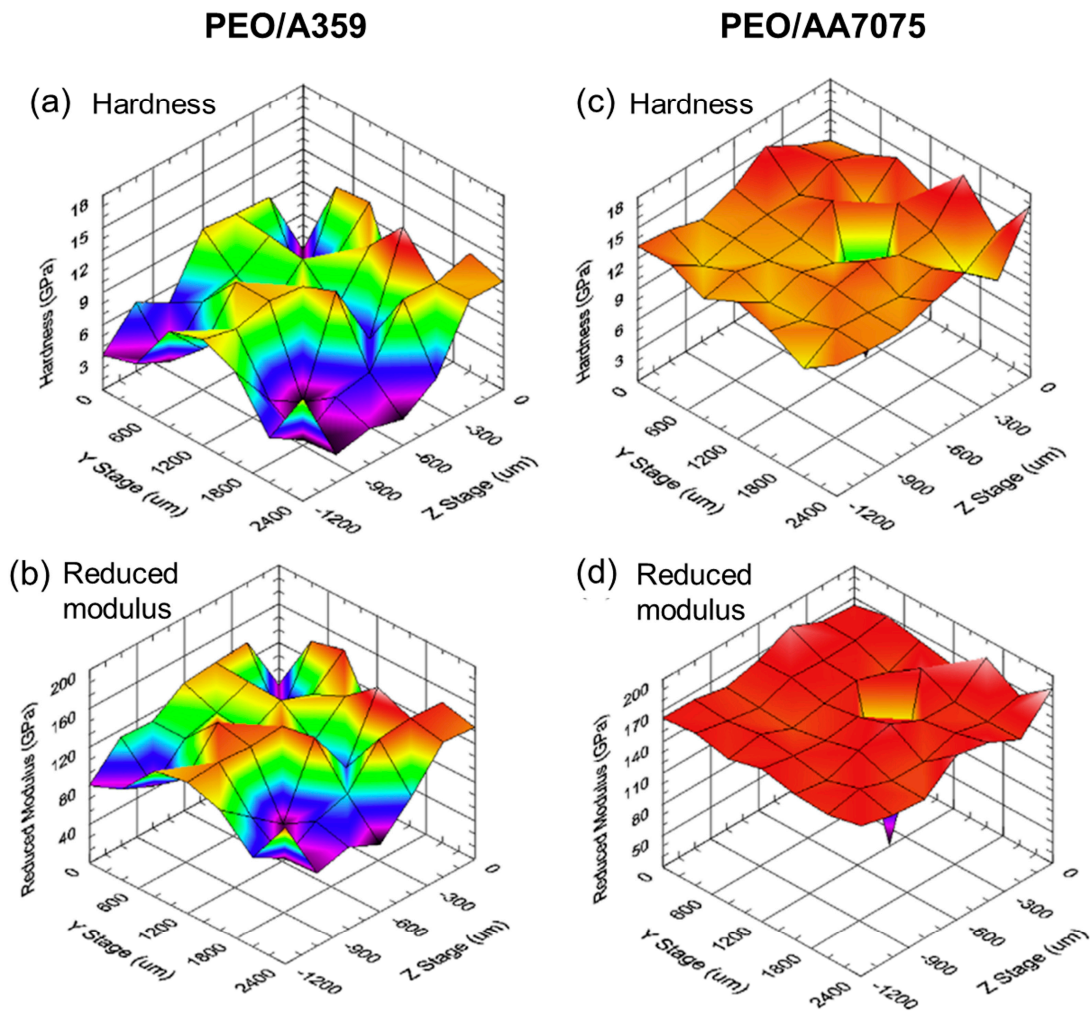


Figure 8. 2D profiles of hardness and reduced modulus of the PEO coatings grown on an A359 (a,b) and AA7075 (c,d) alloys [29]. Reprinted from Materials & Design; 31; G. Sabatini, L. Ceschini, C. Martini, J.A. Williams, I.M. Hutchings; Improving sliding and abrasive wear behaviour of cast A356 and wrought AA7075 aluminium alloys by plasma electrolytic oxidation; 816–828; Copyright (2010), with permission from Elsevier.

Gulec et al. [3] carried out a systematic study to analyze the influence of the Si content on PEO coatings grown on binary cast Al-Si alloys with Si contents between 1% and 32%, by performing PEO processes of 120 min with a silicate-based electrolyte. The researchers observed that, as the Si content increased, the thickness of the developed PEO coating decreased. In addition, α -Al₂O₃ phases were only observed for the alloys containing 1 and 2 at. % Si. Furthermore, it was observed that as the Si content of the alloy increased, the coatings had a smoother appearance and lower roughness, which would be explained by the fact that the melting temperature of SiO₂ (1726 °C) is lower than the melting temperatures of mullite (1828 °C) and Al₂O₃ (2054 °C). The alloys with higher Si content will contain a higher relative amount of Si in the coating, decreasing the melting temperature of the mixed oxides that form the coating, and thus leading to an increase in the fluidity of the materials transported through the plasma channels, covering all the surfaces of the coating as they are sprayed outwards. In addition, the plasma microarcs occurring during the treatment of alloys with higher Si content are weaker, also favoring the formation of coatings with lower porosity and roughness.

Rogov et al. [28] studied the influence of the microstructure of Al-Si substrates on the PEO coating development, by comparing a cast Al-12Si alloy against an Al alloy with a 12% Si content fabricated by additive manufacturing. In this study, an electrolyte composed of 10 g·L⁻¹ Na₂SiO₃ and 2 g·L⁻¹ KOH and a pulsed bipolar power source were employed. Since the cathodic polarization could suppress the passivation of the Si grains, the authors designed a specific wave regime, where only anodic polarization was applied in the first 3 min of the process. After that time, and once the plasma was stably initiated, authors alternated bipolar and unipolar polarization cycles with cathode-only pulses. Their findings suggested that the microstructure of the alloy, i.e., the size and distribution of the Si grains in the metal substrate, had only influenced the most unstable stages of the PEO process: the initial stage and the stage of transition to the soft sparking regime. Once the corresponding micro-discharge regime has been initiated, the process proceeds normally for both alloys.

In a recent paper [25], PEO processes under pulsed bipolar current (PBC) and pulsed bipolar voltage (PBV) modes were performed on pure Al and binary Al-Si alloys with different Si contents (5 wt.% Si, 9 wt.% Si, 12 wt.% Si, and 15 wt.% Si). While under the PBC regime, the Si phases were rapidly oxidized, obtaining similar final thicknesses regardless of the Si concentration of the alloy, under the PBV regime, the Si phases were oxidized more slowly, which was reflected in a lower final thickness on the substrate with higher Si content. The growth of PEO coatings on Al-Si binary alloys was also investigated by Moshrefifar et al. [173], who in their study worked with Al-xSi alloys (x = 1 wt.%, 3 wt.%, 5 wt.%, 7 wt.%, 9 wt.%, 11 wt.%, and 13 wt.%) (Figure 9), obtaining the PEO coatings by using a Na₂SiO₃·5H₂O-containing electrolyte, with and without being modified with Na₂WO₄·2H₂O. As expected, it was observed that a higher Si content in the substrate led to a reduction in the size of the α -Al dendrites and an increase in the eutectic phase (Figure 9). It was reported that a higher porosity percentage and a lower average thickness were attributed to an increased Si content on the substrate. Nevertheless, the higher thicknesses obtained in the samples with lower Si contents presented greater outer layers, which normally exhibit poorer tribological properties than the dense inner layers typically observed in PEO coatings. Thus, the PEO coatings grown in the samples with lower wt.% Si presented higher wear rates, volume losses, and wear track widths (Figure 10). In a further attempt to improve the durability of a PEO coating developed on a cast Al-Si alloy, Student et al. found that the uneven growth of the PEO layers was due to the silicon crystals hindering the proper development of the coatings (Figure 11). The addition of H₂O₂ to the electrolyte significantly enhanced wear resistance by promoting the formation of high-temperature phases like α -Al₂O₃ and 3Al₂O₃·2SiO₂, resulting in increased durability.

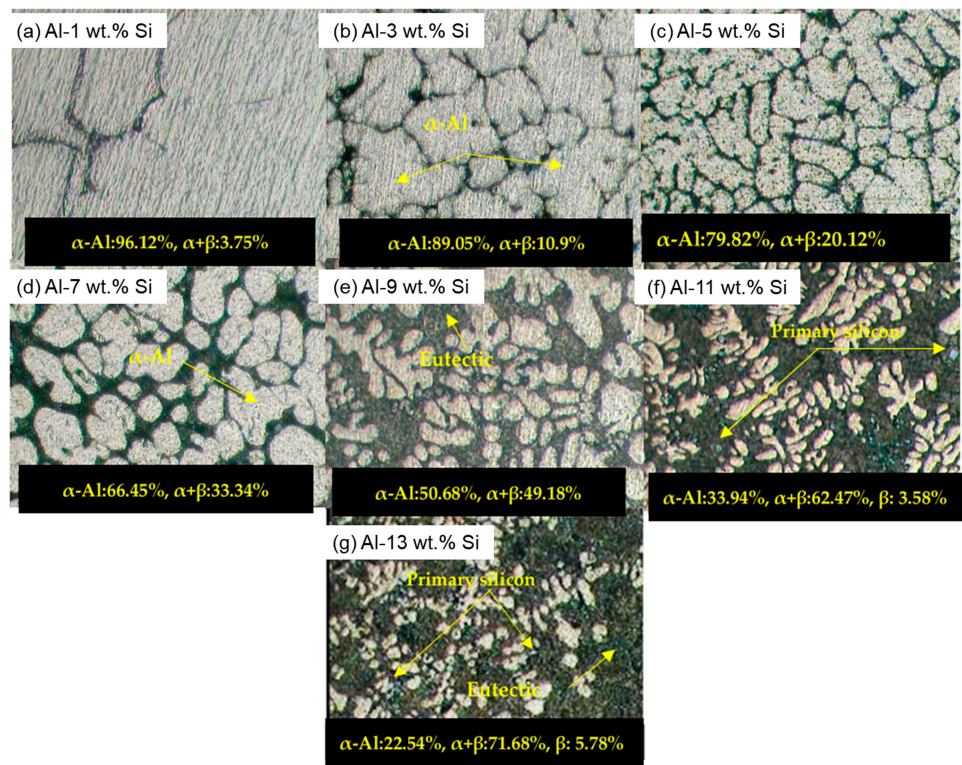


Figure 9. Optical images and each corresponding phase’s percentage of the different Al-Si alloys PEO treated in reference: [173]. Reprinted from <https://www.mdpi.com/2079-6412/12/10/1438>, accessed on 27 December 2023: open access article distributed under the terms and conditions of the Creative Commons Attribution (CC BY) license (<https://creativecommons.org/licenses/by/4.0/>, accessed on 27 December 2023).

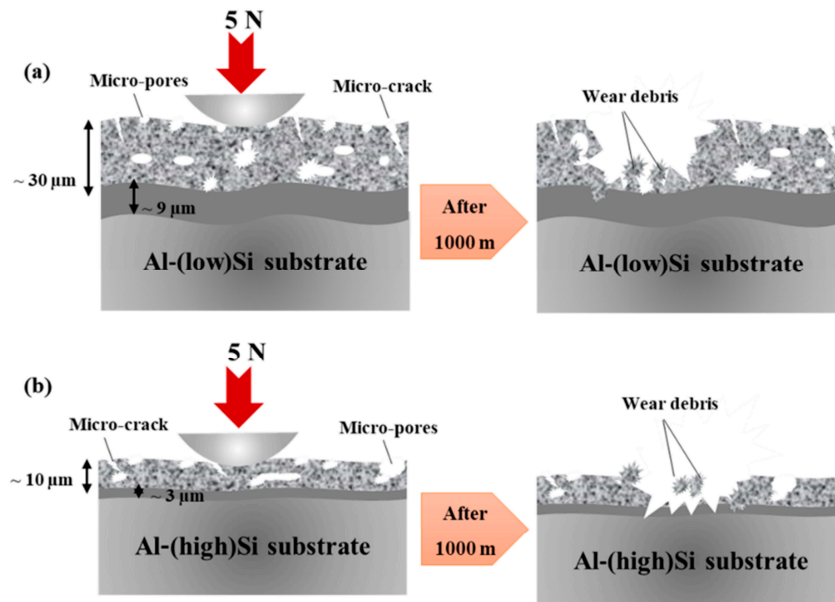


Figure 10. Schematic representation of the wear mechanism of PEO coatings developed on two different Al-Si alloys with low Si content (a) and high Si content (b) [173]. Reprinted from <https://www.mdpi.com/2079-6412/12/10/1438>, accessed on 27 December 2023: open access article distributed under the terms and conditions of the Creative Commons Attribution (CC BY) license (<https://creativecommons.org/licenses/by/4.0/>, accessed on 27 December 2023).

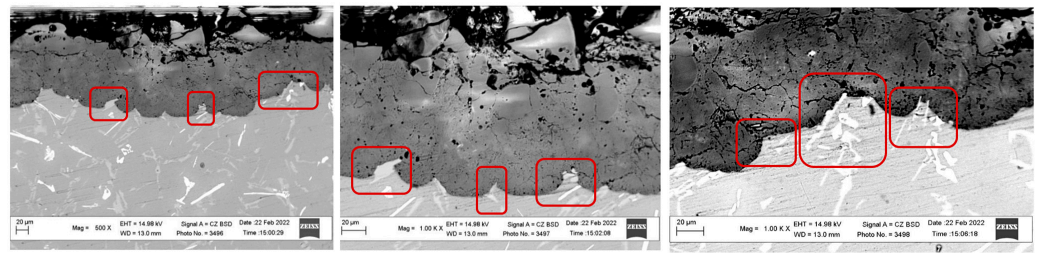


Figure 11. SEM micrographs revealing the cross-section of a PEO coating grown on a cast AlSi10 (AK9) alloy. The marked areas reveal the deceleration in the coating growth in the areas containing Si-rich crystals. Figure adapted from [174]. Reprinted from <https://www.mdpi.com/2079-6412/13/3/637>, accessed on 27 December 2023, open access article distributed under the terms and conditions of the Creative Commons Attribution (CC BY) license (<https://creativecommons.org/licenses/by/4.0/>), accessed on 27 December 2023).

The manufacturing method is also a determinant of the behavior of PEO coatings grown on Al-Si alloys. Mora-Sanchez et al. compared the growth and properties of PEO coatings grown on a conventional A361 cast alloy and on an AM) Al10SiMg alloy, using a silicate-based electrolyte [175]. Compared with the PEO grown on the AM/Al-Si substrate, the PEO coating developed on the cast Al-Si alloy showed finer and lower porosity percent. Nevertheless, the interface between the substrate and the coating was flatter for the AM substrate, since it presented a finer distribution of silicon in comparison with the cast alloy. As referenced in their works, Pezzato et al. [176,177] have demonstrated substantial enhancements in the corrosion resistance of PEO coatings applied on AM AlSi10Mg alloys, obtained by selective laser melting (SLM), in comparison to PEO coatings grown on conventionally cast AlSi10Mg substrate. In both cases, the PEO processes were carried out using a silicate-based electrolyte composed of 25 g/L of Na_2SiO_3 and 2.5 g/L of NaOH. The improved anti-corrosion performance was attributed to the more uniformly distributed Si phases present on the AM Al-Si substrates. Additionally, the absence of Fe and Mn intermetallic compounds contributed to the formation of denser and more uniformly structured PEO coatings.

3.2. PEO Coatings Developed on Cast Al-Si Alloys Using Phosphate-Based Electrolytes

The effect of the addition of NH_4VO_3 to a phosphate-based electrolyte in a PEO process on a cast Al-12Si alloy was studied by Hwang et al. [166]. It was observed that the addition of NH_4VO_3 influenced the size and duration of the plasma micro-discharges, resulting in a decrease in the breakdown voltage. Furthermore, the NH_4VO_3 -containing electrolyte not only promoted a more uniform PEO coating, preventing the heterogeneous growth observed in previous studies, but also led to black PEO coatings. NH_4VO_3 was newly employed for the development of black PEO coatings on a hypoeutectic Al-Si alloy, in combination with Na_2WO_4 , which is a reagent that is also a coating darkener [164]. In this study, the authors found the optimal ratio between the concentrations of Na_2WO_4 and NH_4VO_3 added to a phosphate-based electrolyte to obtain smoother and darker-colored coatings. The formation of vanadium and tungsten oxides in the coating was found to be responsible for the black color. In addition, it was found that the NH_4VO_3 reagent played the most significant role in the formation of the dark-colored coating.

In 2018, Yu et al. treated a eutectic cast Al-Si alloy using a phosphate-based electrolyte [27]. The PEO processes were performed at a low current density, between 4 and $6 \text{ A}\cdot\text{dm}^{-2}$, and resulted in low-thickness PEO coatings (8–10 μm), in which no $\alpha\text{-Al}_2\text{O}_3$ phase was detected. In this study, the authors proposed a new and interesting model to explain the growth mechanism of the PEO coating on a cast Al-Si alloy, which contradicts the theory proposed by Wang & Nie [171]. According to Wang & Nie, after the initial passivation stage, discharges occurred at the edge between Al and Si, due to the border effect promoted by the occurrence of a critical potential value due to the electrical concentration at

that interface. Furthermore, Wang & Nie suggested that during passivation, the film grows inward, whereas when Al or Si oxides are formed, there would be some expansion in the volume of the formed layer. According to Yu et al. [27], the thickness of the layer created during the initial passivation stage (in the order of nanometers) is significantly lower than the roughness of the substrate (in the order of microns). Thus, these authors believed that the boundary effect prevented the initiation of discharges and proposed a new growth mechanism consisting of three steps: passivation, stable oxidation, and final oxidation stages. According to this novel model, during the passivation stage, which occurs before the potential reaches the dielectric breakdown value, anodic layers grow on both the Al matrix and the Si crystals (Figure 12 I). Since it is a very quick stage, the authors suggested that the thickness of the anodic layers grown on the Al and Si phases should have a similar thickness. In the stage of stable oxidation, once the breakdown potential has been exceeded, the anodic layers break down and the plasma microdischarges appear. The first areas of the anodic layers to be broken and where the plasma discharges will appear are those of Al_2O_3 formed on the Al matrix, since this oxide has a lower dielectric strength than SiO_2 (Figure 12 II) [27]. Due to the high temperature caused by the discharges, the area where the point discharge occurs is melted, further oxidizing the underlying Al matrix. At the end of the discharge, the molten oxide solidifies, due to the lower temperature of the electrolyte, rebuilding the film at that point. This process is repeated in the areas above the Al matrix, thereby creating the coating. Furthermore, as the coating grows, the discharge potential increases, corresponding to the increase in potential shown in stages II and III of Figure 4. Once the discharge voltage exceeds the value of the SiO_2 films grown on the Si phases of the alloy, discharge points start to occur in these areas as well. These new discharges start at the edges of the larger Si particles since a larger area is in contact with the Al matrix, which has far higher conductivity than Si. Through oxidation and diffusion, Al-Si-O oxides form and, as these films grow, the discharges move towards the center of the Si phases. For the smaller Si particles, the Al-Si-O layers tend to form directly, as discharges occur over their entire surface (Figure 12 III). This process is repeated, increasing the thickness of the coating and reaching the final oxidation stage. However, the discharges mostly occur in the Al_2O_3 -rich areas, as the discharge voltage in these areas is lower than in the SiO_2 areas (Figure 12 IV), which cause the thickness of the coating on the Si particles to be slightly lower than that grown on the Al matrix. At this stage, in the areas where there are small, oxidized Si particles, the Al matrix underneath is oxidized, as well as small Si particles that are immersed in the oxidizing Al matrix. These processes promote the reactions between Al_2O_3 and SiO_2 , including the formation of aluminosilicates [27].

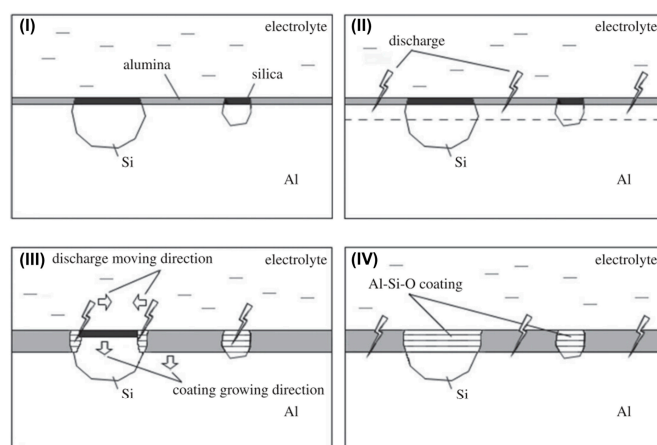


Figure 12. Schematic representation of the coating growth mechanism, with the stages I, II, III and IV described above, proposed by Yu et al. [27]. Reprinted from <https://royalsocietypublishing.org/doi/10.1098/rsos.172428>, accessed on 27 December 2023: open access article published by the Royal Society under the terms on the Creative Commons Attribution License <http://creativecommons.org/licenses/by/4.0/4.0/> (accessed on 27 December 2023), which permits unrestricted use.

The influence of the secondary phases Al_2Cu , $\beta\text{-Al}_5\text{FeSi}$ and eutectic Si present in an AlSi9Cu3 alloy, on the formation and growth of the PEO coating, was investigated by Wu et al. [47]. In their study, they carried out several PEO processes with durations ranging from 15 to 480 s, using an electrolyte composed of Na_3PO_4 and KOH and a unipolar-pulsed DC power supply. In this research, it was observed that the electrical field-assisted dissolution occurring at the beginning of the PEO process begins at the interface between the Al_2Cu intermetallics and the $\alpha\text{-Al}$ matrix. The reason for this was that these intermetallic phases presented a native oxide layer of lower coverage than the one formed spontaneously on the $\alpha\text{-Al}$ matrix, so the Al_2Cu particles were more exposed to the electrolyte, thus forming at these interfaces low soluble Al/Cu-based oxides and phosphates. Regarding the $\beta\text{-Al}_5\text{FeSi}$ intermetallic, Fe tends to create defects and paths through which the electrolyte can penetrate, while due to its higher resistivity, Si tends to change the current flow, both resulting in a lower oxidation rate compared to the Al_2Cu intermetallic. As the coating thickness increased, the films grown on the Al_2Cu and $\beta\text{-Al}_5\text{FeSi}$ intermetallics tended to overlap, presenting a more porous and less dense morphology than that formed on the Al matrix, while on the eutectic Si particles, the thinner films with cracks were formed. The sequence in which the coating was formed on this alloy was the $\alpha\text{-Al}$ matrix, Al_2Cu , $\beta\text{-Al}_5\text{FeSi}$, and eutectic Si.

3.3. PEO Coatings Developed on Cast Al-Si Alloys Using Aluminate-Based Electrolytes

After an in-depth study of the coating growth mechanism with silicate-based electrolytes, the conventional electrolytes most widely applied in this technology, and studies carried out with phosphate-based electrolytes, the use of aluminate-based electrolytes for the PEO treatment of cast Al-Si alloys was also investigated. Among other reasons, it had previously been observed that aluminate-based electrolytes used in Al alloys provided coatings with higher resistance than those obtained using silicate-based electrolytes [136]. In this context, Xie et al. studied for the first time the use of aluminate-based electrolytes in the PEO treatment of a cast A356 Al-Si alloy [54]. In their research, authors used pulsed bipolar polarization regimes with constant current, and analyzed the effect of NaAlO_2 concentration in the electrolyte, using solutions containing $2\text{ g}\cdot\text{L}^{-1}$, $16\text{ g}\cdot\text{L}^{-1}$, and $24\text{ g}\cdot\text{L}^{-1}$ NaAlO_2 and $1\text{ g}\cdot\text{L}^{-1}$ KOH, and compared these electrolytes against one composed of $8\text{ g}\cdot\text{L}^{-1}$ Na_2SiO_3 + $1\text{ g}\cdot\text{L}^{-1}$ KOH. The electrolyte composed of $24\text{ g}\cdot\text{L}^{-1}$ NaAlO_2 provided coatings with a monolayer structure and the presence of $\alpha\text{-Al}_2\text{O}_3$ phases, giving the best wear and corrosion behavior and improving the results obtained with the conventional silicate-based electrolyte.

Since the best results in the previous study were obtained with the more concentrated electrolyte, Cheng et al. investigated the use of an electrolyte consisting of $32\text{ g}\cdot\text{L}^{-1}$ NaAlO_2 in the PEO treatment of alloy A356 [125]. However, the use of highly concentrated aluminate-based electrolytes can lead to instability and precipitation of the solution, which would be detrimental during PEO treatment. NaOH is a reactant that can improve the stability of the electrolyte, making it more durable, although if the amount of NaOH added is excessive, the electrolyte would become corrosive and detrimental to the PEO process. In this regard, the addition of $1\text{ g}\cdot\text{L}^{-1}$, $5\text{ g}\cdot\text{L}^{-1}$, and $10\text{ g}\cdot\text{L}^{-1}$ NaOH to the electrolyte with $32\text{ g}\cdot\text{L}^{-1}$ NaAlO_2 and its effects on the properties of the developed coatings were studied. Cheng et al. [125] observed that increasing the NaOH concentration from 1 to $5\text{ g}\cdot\text{L}^{-1}$ increased the storage time of the electrolyte under good conditions from 1 day to at least 35 days, and this improvement was even greater when the NaOH concentration was $10\text{ g}\cdot\text{L}^{-1}$. However, for the PEO process, the use of an electrolyte with such a high NaAlO_2 concentration requires the application of a PEO pre-treatment using an electrolyte with a lower NaAlO_2 concentration for the formation of the passive layer necessary for the initiation of the plasma discharges, which cannot form by itself when the electrolyte is too concentrated due to excessive dissolution of the metal substrate. Thus, although increasing the NaOH concentration improved the stability of the electrolyte, it also required a significantly longer pre-treatment, which would not be practical on an industrial scale due

to the increased time and energy costs. Therefore, the authors concluded that the electrolyte offering the best compromise between all requirements, both in terms of stability and coating performance, was the electrolyte composed of $32 \text{ g}\cdot\text{L}^{-1}$ NaAlO_2 and $5 \text{ g}\cdot\text{L}^{-1}$ NaOH .

Fernández-López et al. [4] developed and characterized the PEO coatings grown on a secondary cast Al-Si alloy (EN AC 46-500) using two novel aluminate-based electrolytes whose main component was NaAlO_2 , while the effect of the addition of K_2TiF_6 was also evaluated. Compared to the uncoated cast Al-Si reference, the novel coatings showed a remarkable increase in hardness (with values around $1600 \text{ HV}_{0.025}$), as well as a high coating growth rate, corresponding to $1 \mu\text{m}\cdot\text{min}^{-1}$ and $1.41 \mu\text{m}\cdot\text{min}^{-1}$ for coatings obtained using the electrolytes without and with K_2TiF_6 , respectively. The tribological analysis of the PEO coatings showed a very stable evolution of friction during the wear tests and a notable reduction of the wear rates compared to the base material (Figure 13). Moreover, the novel PEO coatings also provided an enhancement in corrosion protection compared to the uncoated reference. The most promising results, both in terms of tribology and corrosion protection, were obtained with the PEO coatings developed using the aluminate-based electrolyte containing K_2TiF_6 [4].

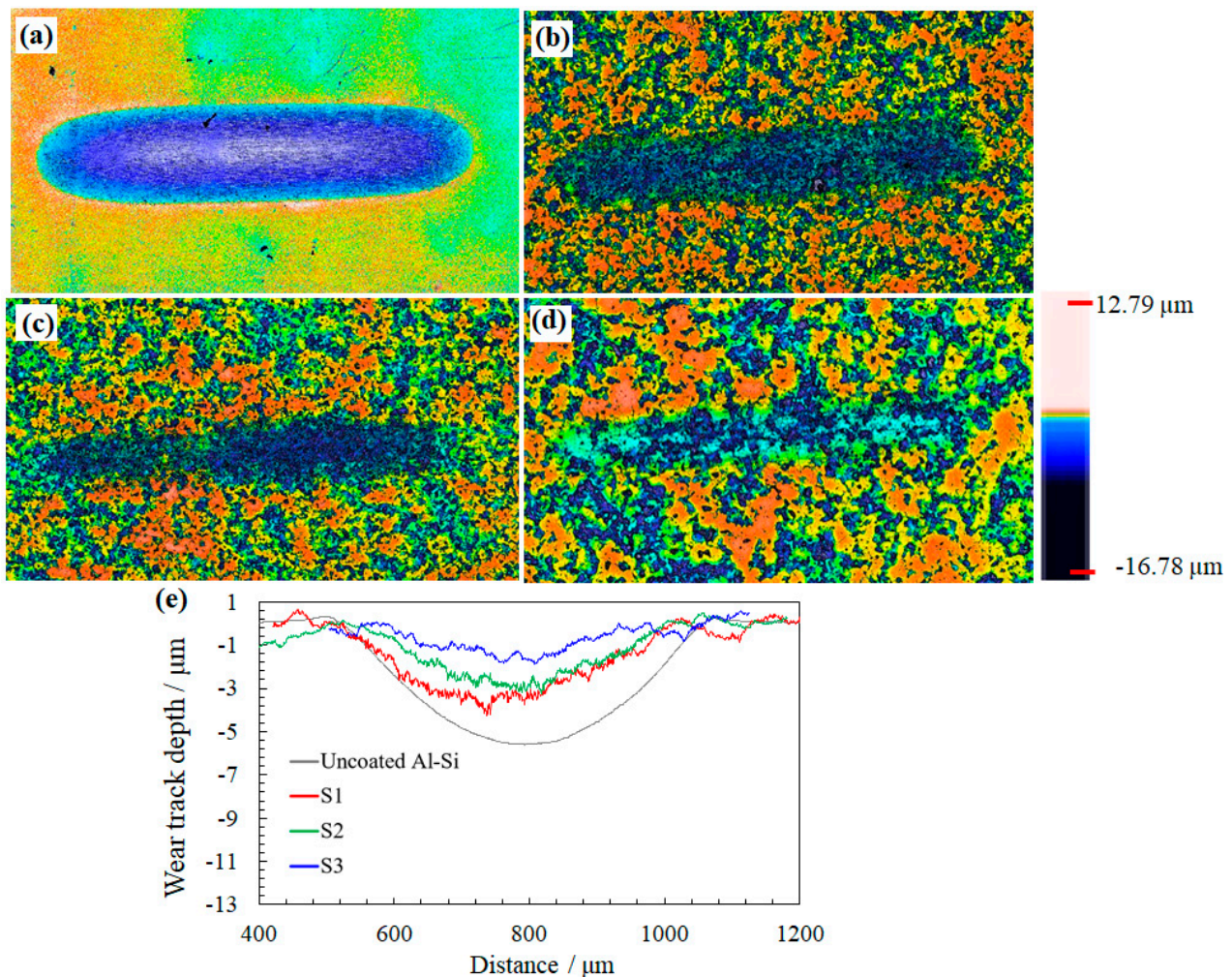


Figure 13. 3D displays of the wear tracks after the tribological tests: uncoated cast Al-Si alloy (a), PEO coatings developed using the aluminate-based electrolyte without thermal treatment (b) and with thermal treatment (c), the aluminate-based electrolyte additivated with K_2TiF_6 (d), and corresponding wear depth profiles along the whole width scar (e) [4]. Reprinted from Ceramics International; 47; P. Fernández-López, S.A. Alves, A. López-Ortega, J.T. San José-Lombera, R. Bayón; High performance tribological coatings on a secondary cast Al-Si alloy generated by Plasma Electrolytic Oxidation; 31238–31250; Copyright (2021), with permission from Elsevier.

The tribological behavior of PEO-coated high-Si cast Al-Si cylinder liners was recently investigated by Alves et al. [23]. The novel PEO coating was successfully grown on the hypereutectic cylinder liners obtained using the aluminate-based electrolyte formulated in [4]. It was thoroughly evaluated and compared with a PEO coating grown using a commercial silicate-based electrolyte, also additivated with BN nanoparticles. The findings revealed that the properties of the PEO coatings were drastically determined by the composition of the electrolyte used during the PEO processes. Thus, the PEO coatings developed using the aluminate-based electrolyte provided a significant improvement in the tribological performance for the studied application (i.e., lower wear damage and lower friction values), which was even comparable to the results provided by the cylinder liners made of cast iron, the conventional material.

Fernández-López et al. [14] successfully developed novel PEO coatings on a recycled cast Al-Si alloy with improved corrosion and tribocorrosion protection. For this purpose, a new aluminate-based electrolyte was developed, which also Na_2WO_4 and K_2TiF_6 . All the elements present in the electrolyte were satisfactorily incorporated into the layer, resulting in a coating composed of several oxides, although its main crystalline component was $\alpha\text{-Al}_2\text{O}_3$ (Figure 14). Another noteworthy finding was obtained with regard to the chemical composition of the two sub-layers that made up the coating, where the analysis revealed a higher Si content in the inner regions, which would come from the metallic substrate, while the higher Al content in the outer region of the coating would mainly come from the aluminate-based electrolyte. It was also observed that the innermost sublayer had a lower density than the outermost one, which would have been caused by the formation of a higher proportion of Si oxides, which are more porous than Al oxides, in the areas adjacent to the substrate [14].

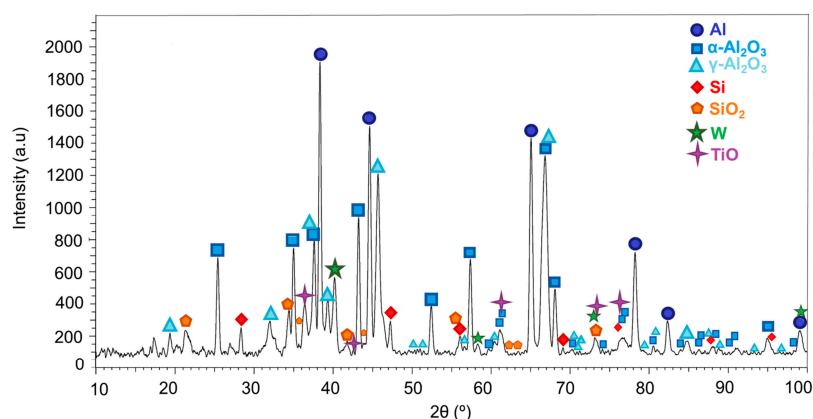


Figure 14. XRD pattern obtained for the PEO coating grown on a secondary cast Al-Si alloy [14]. Reprinted from Corrosion Science; 207; Patricia Fernández-López, Sofia A. Alves, Itziar Azpitarte, José T. San-José, Raquel Bayón; Corrosion and tribocorrosion protection of novel PEO coatings on a secondary cast Al-Si alloy: Influence of polishing and sol-gel sealing; 110548; Copyright (2022), with permission from Elsevier.

3.4. Development of High-Performance PEO Coatings on Cast Al-Si Alloys: Other Strategies

Various strategies have been pursued to develop coatings with optimal properties in combination with PEO technology, due to the difficulty of treating cast Al-Si alloys. Among the strategies pursued, pre-treatments, such as thermal, chemical, or electrochemical treatments, post-treatments, such as sealing or adding solid lubricants to the coating, as well as the incorporation of nanoparticles into the electrolyte have been studied.

3.4.1. Pre- and Post-Treatments

Not only can the properties of a PEO coating be modified by its post-treatment, but the application of different treatments to the metallic substrate, prior to the deposition of the coating, will also have a significant influence on the growth and characteristics of the

coating. Heat treatments are one of the most widely performed pre-treatments, leading, among other effects, to the modification and/or homogenization of the microstructure, which will influence the growth rate of the PEO coating, since the different phases of the substrate possess different conducting behaviors. In this context, Krishtal et al. studied the influence of different heat treatments (i.e., T2 and T6), performed on cast Al-Si alloys, on the properties of the obtained PEO coatings. In general terms, it was determined that the coalescence and spheroidization of the silicon phases obtained by the heat treatment decreased the overall electrical resistance of the material, increased the current-carrying areas of the material, and promoted better adhesion between the coating and the matrix than between the coating and the silicon phases. The resulting changes accomplished with the heat treatments promoted the growth of coatings with increased thickness, higher adhesion to the substrate, greater hardness, and enhanced homogeneity and wear resistance [170].

The high silicon content of cast Al-Si alloys constitutes the major impediment to the establishment of a stable discharge regime at the beginning of the PEO process, which consequently promotes coatings with poorer mechanical properties. The application of a chemical etching is an effective strategy to selectively remove the surface of cast alloys with higher silicon content to promote a surface more electrically transparent. Li et al. [178] chemically etched a binary Al-Si12 alloy by immersing the samples in an acidic solution of HNO₃ and HF for 30 s. This pre-treatment favors the establishment of the micro-plasma regime during the process, not only improving the growth rate, but also decreasing energy consumption [178]. Indeed, it was also observed that the acid pre-treatment positively enhanced the evolution of the positive potential at the beginning of the process, increasing the coating growth rate from 0.50 $\mu\text{m}\cdot\text{min}^{-1}$ to 0.84 $\mu\text{m}\cdot\text{min}^{-1}$ [178]. Furthermore, surface etching promoted a decrease in amorphous SiO₂ and mullite in the coatings, as well as an improvement in the energy efficiency of the process, which decreased from 6.30 $\text{kW}\cdot\text{h}\cdot\mu\text{m}^{-1}\cdot\text{m}^{-2}$ to 4.36 $\text{kW}\cdot\text{h}\cdot\mu\text{m}^{-1}\cdot\text{m}^{-2}$. Another research also carried out an acid etching with the main aim of removing the detrimental β -Si phase contained in the skin layer of cast Al alloys with Si contents of 9 wt.%, 12 wt.%, and 15 wt.% [179]. The removal of the β -Si phase from the outermost region of the metallic substrates increased the coating growth rate and energy efficiency during early PEO stages. Extending etching time to 30 s notably improved the anticorrosion properties of the PEO coating on the Al-12Si alloy (Figure 15). Alloys with 60 s of acid etching displayed reduced Si content and larger surface pores, resembling pure Al's behavior within the initial 10 min of oxidation. However, large surface pores were filled by oxides after 30 min of PEO treatment, promoting denser layers.

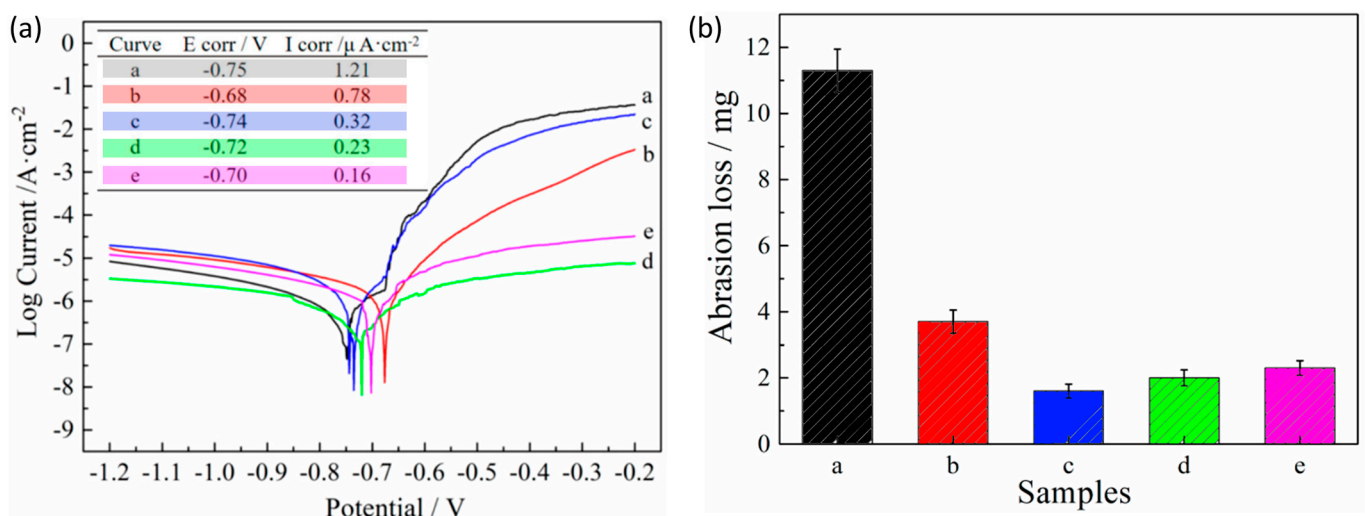


Figure 15. (a) Polarization curves and (b) weight loss evaluated for (a) the Al-12 Si matrix, (b–e) the Al-12 Si alloy subjected to etching durations of 0, 15, 30, and 60 s, respectively, followed by 30 min of PEO treatment.

The effect of refining the silicon phases on the properties of the developed PEO coating was also investigated [180]. For this purpose, a pre-treatment was carried out by adding Sr during the melting process in the fabrication of the cast Al-Si alloy. The pre-treatment effectively modified the silicon particles present in the aluminum matrix, decreasing their size and leading to a more homogeneous distribution of these phases. Consequently, the initial stage of the process was improved, leading to more uniform and thicker coatings. The final modified PEO-treated Al-Si alloys also showed a higher compactness and enhanced corrosion resistance, compared with the non-modified Al-Si substrates.

More demanding environments require the development of high-performance coatings, for which it could be necessary the application of more complex treatments. Mohedano et al. conducted a comprehensive study involving an anodizing pre-treatment and a sealing post-treatment applied to PEO coatings on an A356 alloy, using a silicate-based electrolyte and an AC power source [31]. The anodizing pre-treatment aimed to preserve the original substrate microstructure on cast A356 alloy. However, due to the presence of eutectic phases and intermetallic compounds, hindering the proper growth of the oxide layer, the resulting layers exhibited limitations. Nevertheless, the PEO coatings grown on the pre-anodized samples also exhibited the α -Al₂O₃ phase. The post-treatment involved the sealing of PEO coatings through the immersion of the coated samples on solutions containing salts of Ni (20 min of immersion), Ce (120 min of immersion), phosphonic acid (1440 min of immersion), and KMnO₄ (25 min of immersion). All the sealed samples exhibited not only an enhanced corrosion resistance compared with the unsealed PEO samples, but also improved hydrophobic performance. Shirani et al. developed a duplex coating by burnishing the surface of a PEO coating grown on a cast A356 alloy with graphite-MoS₂-Sb₂O₃ chameleon solid lubricant powder to reduce friction under tribological conditions [55]. The intrinsic morphology of the ceramic layer acted as an optimal supporter of the powder lubricant, while the solid powder applied reduced the surface roughness of the PEO coating. The composite coating exhibited an excellent improvement of the wear resistance, also decreasing the COF by one order of magnitude while showing high thermo-mechanical stability.

Despite the positive results obtained with a new coating developed on a recycled cast Al-Si alloy in terms of growth rate, surface appearance, and density, the typical defects of PEO layers grown on this type of substrates (i.e., high roughness and surface porosity) were still found [14]. In an attempt to improve these intrinsic limitations, the application of two post-treatments, surface polishing and the application of a sol-gel layer, was investigated. The investigated post-treatments proved to be effective in sealing pores and reducing surface roughness, resulting in a significant improvement in the corrosion and tribocorrosion performance of the coating. Nevertheless, the experimental results showed differences in corrosion and tribocorrosion resistance depending on the presence or type of post-treatment applied, and therefore the degradation mechanisms of the different types of materials under the two types of aggressive environments were considered (Figure 16). In particular, the PEO coating sealed with sol-gel proved to be more effective in terms of anti-corrosion resistance, while the polishing of the outer porous layer favored a better tribological behavior in corrosive environments [14].

3.4.2. Nanoparticles Addition

Adding nanoparticles to the electrolytes to be incorporated into the coating during the process was another strategy used to improve the properties of PEO coatings grown on cast Al-Si alloys.

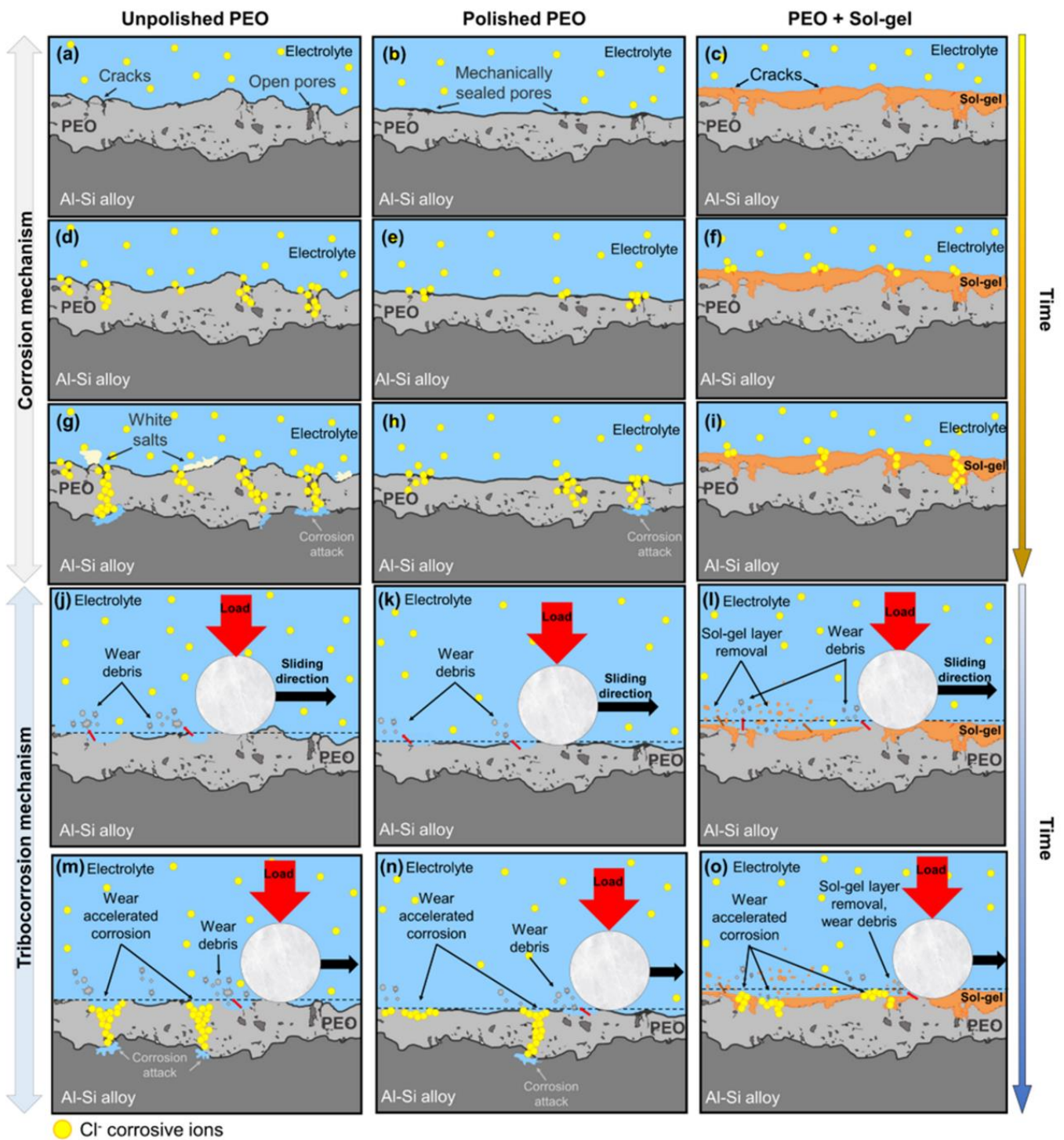


Figure 16. Corrosion (a–i) and tribocorrosion (j–o) mechanisms corresponding to the PEO coatings with different post-treatments [14]. Reprinted from Corrosion Science; 207; Patricia Fernández-López, Sofia A. Alves, Itziar Azpitarte, José T. San-José, Raquel Bayón; Corrosion and tribocorrosion protection of novel PEO coatings on a secondary cast Al-Si alloy: Influence of polishing and sol–gel sealing; 110548; Copyright (2022), with permission from Elsevier.

The incorporation of ZrO_2 into porous ceramic coatings on Al alloys improves tribological behavior by increasing the hardness of the coating and its corrosion resistance. Hu et al. added NH_4VO_3 and 200 nm ZrO_2 nanoparticles to a Na_2SiO_3 and NaOH electrolyte and studied the individual effect of each reagent on the properties of a coating grown on an Al-10Si alloy, obtained by pulsed bipolar polarization [181]. It was observed that the silicate-based electrolyte containing NH_4VO_3 resulted in an aesthetic and dark coating, but the coating exhibited poor tribological behavior. However, the addition of ZrO_2 nanoparticles to the electrolyte maintained the smooth and dark coating surface, but also reduced its surface roughness and improved its hardness, which enhanced its tribological behavior. In another study, ZrO_2 was newly incorporated into a silicate-based electrolyte with the aim of improving the properties of a PEO coating obtained on an Al-12Si cast piston [62]. In this case, it was observed that the ZrO_2 sol promoted further growth of the coating by weakening the inhibitory behavior of the Si phases while obtaining a coating with improved compactness. In addition, good thermal shock resistance results were also obtained, as the coating withstood 1000 thermal shock cycles without showing any surface cracks.

Besides ZrO_2 nanoparticles, the effect on the PEO treatment of an A356 alloy after the addition of titanium carbide (TiC) nanoparticles in two different electrolytes, containing $N_4P_2O_7^-$ and Na_2SiO_3 , was also studied [182]. These nanoparticles, with a size below 200 nm, were incorporated by an inert mechanism, without any chemical reaction during the process. Polunin et al. achieved excellent results with the addition of TiC nanoparticles: not only the hardness and elastic modulus of the coatings were increased, but also the wear and corrosion resistance were improved by a factor of 3 and 10, respectively [182]. The effect of SiO_2 nanoparticles, with average sizes of 48 nm and 100 nm, on the PEO treatment of an A361 Al-Si alloy was further investigated [183]. The SiO_2 nanoparticles of smaller size, 48 nm, were more effectively incorporated into the PEO coatings, which also showed a finer microstructure. Compared to the coatings developed with the electrolyte without nanoparticles, the additivated electrolytes led to an improved oxidability during the processes, which promoted the development of coatings with increased thickness, which also showed a significant improvement in wear and thermal resistance.

4. Conclusions

Cast Al-Si alloys are a versatile material of great interest for many applications, highlighting their use in the automotive industry. However, their applications require the fulfillment of demanding requirements, which often require the surface enhancement of these Al alloys. In this context, a thorough understanding of the capabilities, limitations, and comparative advantages of PEO over conventional treatments such as anodizing is required.

The present work constitutes a comprehensive review concerning the development of ceramic coatings on cast Al-Si alloys using plasma electrolytic oxidation (PEO) technology. While anodizing has long been an established practice for the modification of Al alloys, PEO has emerged as a promising technology due to its distinctive characteristics, including the ability to produce thicker, more adherent coatings with increased wear and corrosion resistance, thereby positioning it as an attractive alternative. Furthermore, PEO is a more versatile technology, with a lower dependence on the substrate composition and morphology. These characteristics are particularly relevant for the surface treatment of cast Al-Si alloys, whose inherent complex microstructure has significantly hindered their anodizing and, consequently, requires novel solutions to meet the challenges arising from their singular morphology. The understanding behind the details of PEO technology, covering the coating growth mechanisms and the critical process parameters, highlights the significance of substrate composition, electrolyte formulation, and power supply selection for achieving optimal results. The systematic screening of the electrolyte types (including silicate-, phosphate-, and aluminate-based formulations), has led to a better understanding of the suitability of the development of PEO coatings for cast Al-Si alloys, with each type of formulation offering different advantages and challenges.

Innovative strategies for further enhancing PEO coatings on cast Al-Si alloys have been also discussed in this review. The analysis of the results obtained after the application of different pre- and post-treatments and the dispersion of nanoparticles into the electrolytes highlighted their potential for the optimization of the PEO coatings performance, while also addressing some of the inherent challenges associated with these coatings.

To conclude, PEO technology is proving to be a promising path for the improvement of the performance of cast Al-Si alloys, which are widely employed in the automotive sector, and a growing number of scientific publications based on this subject have been published in recent years. The identification of the fundamental understanding of PEO technology, the discussion about the influence of the chemical composition of the electrolyte, and the analysis of some innovative strategies for the surface treatment of these materials carried out in this work could provide a basis for the ongoing research efforts.

5. Future Perspective and Remarks

This comprehensive review underscores the need for continued research and innovation in the field of surface modification of cast Al-Si alloys. While the introduction of PEO technology has shown great potential, there are still interesting avenues for further exploration. Further research should prioritize the optimization of PEO coatings to address the specific challenges associated with cast Al-Si alloys. This requires a deeper understanding of the interaction between the composition of the electrolyte, process parameters, and substrate morphology in order to develop coatings with improved performance.

To summarize, while PEO technology offers significant opportunities for enhancing cast Al-Si alloys, continued interdisciplinary collaboration and exploration are essential to achieve optimal coatings that meet the needs of diverse applications in the automotive sector and beyond.

Funding: The authors would like to acknowledge the Department of Education, Linguistic Policy and Culture of the Basque Government for its support through the grant “Programa Predoctoral de Formación de Personal Investigador No Doctor (2022–2023)” awarded to the first author.

Institutional Review Board Statement: Not applicable.

Informed Consent Statement: Not applicable.

Data Availability Statement: Data are contained within the article.

Conflicts of Interest: The authors declare no conflicts of interest.

References

1. Robles Hernandez, F.C.; Herrera Ramírez, J.M.; Mackay, R. *Al-Si Alloys: Automotive, Aeronautical, and Aerospace Applications*; Springer: Berlin/Heidelberg, Germany, 2017; ISBN 9783319583792.
2. Ervina Efzan, M.N.; Kong, H.J.; Kok, C.K. Review: Effect of Alloying Element on Al-Si Alloys. *Adv. Mater. Res.* **2014**, *845*, 355–359. [[CrossRef](#)]
3. Gulec, A.E.; Gencer, Y.; Tarakci, M. The Characterization of Oxide Based Ceramic Coating Synthesized on Al-Si Binary Alloys by Microarc Oxidation. *Surf. Coat. Technol.* **2015**, *269*, 100–107. [[CrossRef](#)]
4. Fernández-López, P.; Alves, S.A.; López-Ortega, A.; San José-Lombera, J.T.; Bayón, R. High Performance Tribological Coatings on a Secondary Cast Al-Si Alloy Generated by Plasma Electrolytic Oxidation. *Ceram. Int.* **2021**, *47*, 31238–31250. [[CrossRef](#)]
5. Glazoff, M.V.; Khvan, A.V.; Zolotarevsky, V.S.; Belov, N.A.; Dinsdale, A.T. *Industrial and Perspective Casting Alloys*; Elsevier: Amsterdam, The Netherlands, 2019; ISBN 9780128118054.
6. Zamani, M. Al-Si Cast Alloys—Microstructure and Mechanical Properties at Ambient and Elevated Temperature Al-Si Cast Alloys—Microstructure and Mechanical Properties at Ambient and Elevated Temperature. Ph.D. Thesis, Jönköping University, Jonkoping, Sweden, 2015.
7. Kumar, L.; Jang, J.C.; Yu, H.; Shin, K.S. Effect of Secondary Phase on Mechanical and Thermal Conductivity of Al-Si-XFe-Mg-YCu-Mn Die Casting Alloys. *Mater. Lett.* **2022**, *314*, 131889. [[CrossRef](#)]
8. Shabestari, S.G. The Effect of Iron and Manganese on the Formation of Intermetallic Compounds in Aluminum-Silicon Alloys. *Mater. Sci. Eng. A* **2004**, *383*, 289–298. [[CrossRef](#)]
9. Otani, L.B.; Soyama, J.; Zepon, G.; Costa e Silva, A.; Kiminami, C.S.; Botta, W.J.; Bolfarini, C. Predicting the Formation of Intermetallic Phases in the Al-Si-Fe System with Mn Additions. *J. Phase Equilibria Diffus.* **2017**, *38*, 298–304. [[CrossRef](#)]

10. Cao, X.; Saunders, N.; Campbell, J. Effect of Iron and Manganese Contents on Convection-Free Precipitation and Sedimentation of Primary α -Al(FeMn)Si Phase in Liquid Al-11.5Si-0.4Mg Alloy. *J. Mater. Sci.* **2004**, *39*, 2303–2314. [[CrossRef](#)]
11. Rams, J.; Torres, B. Casting Aluminum Alloys. *Encycl. Mater. Met. Alloy.* **2021**, *1*, 123–131. [[CrossRef](#)]
12. Berlanga-Labari, C.; Biezma-Moraleda, M.V.; Rivero, P.J. Corrosion of Cast Aluminum Alloys: A Review. *Metals* **2020**, *10*, 1384. [[CrossRef](#)]
13. Yu, W.; Zhao, H.; Wang, L.; Guo, Z.; Xiong, S. The Influence of T6 Treatment on Fracture Behavior of Hypereutectic Al-Si HPDC Casting Alloy. *J. Alloys Compd.* **2018**, *731*, 444–451. [[CrossRef](#)]
14. Fernández-López, P.; Alves, S.A.; Azpitarte, I.; San-José, J.T.; Bayón, R. Corrosion and Tribocorrosion Protection of Novel PEO Coatings on a Secondary Cast Al-Si Alloy: Influence of Polishing and Sol-Gel Sealing. *Corros. Sci.* **2022**, *207*, 110548. [[CrossRef](#)]
15. Wang, D.; Zhang, X.; Nagaumi, H.; Li, X.; Zhang, H. 3D Morphology and Growth Mechanism of Cubic α -Al(FeMnCr)Si Intermetallic in an Al-Si Cast Alloy. *Mater. Lett.* **2020**, *277*, 128384. [[CrossRef](#)]
16. Xue, W.; Wang, C.; Li, Y.; Chen, R.; Zhang, T. Analyses of Microarc Oxidation Coatings Formed on Si-Containing Cast Aluminum Alloy in Silicate Solution. *ISIJ Int.* **2002**, *42*, 1273–1277. [[CrossRef](#)]
17. Peppas, A.; Kollias, K.; Dragatogiannis, D.A.; Charitidis, C.A. Sustainability Analysis of Aluminium Hot Forming and Quenching Technology for Lightweight Vehicles Manufacturing. *Int. J. Thermofluids* **2021**, *10*, 100082. [[CrossRef](#)]
18. Li, X.; Nie, X.; Wang, L.; Northwood, D.O. Corrosion Protection Properties of Anodic Oxide Coatings on an Al-Si Alloy. *Surf. Coat. Technol.* **2005**, *200*, 1994–2000. [[CrossRef](#)]
19. Gonçalves, M.; Monteiro, H.; Iten, M. Life Cycle Assessment Studies on Lightweight Materials for Automotive Applications—An Overview. *Energy Rep.* **2022**, *8*, 338–345. [[CrossRef](#)]
20. Luo, A.A.; Sachdev, A.K.; Apelian, D. Alloy Development and Process Innovations for Light Metals Casting. *J. Mater. Process. Technol.* **2022**, *306*, 117606. [[CrossRef](#)]
21. Zhang, W.; Xu, J. Advanced Lightweight Materials for Automobiles: A Review. *Mater. Des.* **2022**, *221*, 110994. [[CrossRef](#)]
22. Javidani, M.; Larouche, D. Application of Cast Al-Si Alloys in Internal Combustion Engine Components. *Int. Mater. Rev.* **2014**, *59*, 132–158. [[CrossRef](#)]
23. Alves, S.A.; Fernández-López, P.; López-Ortega, A.; Fernández, X.; Quintana, I.; San-José, J.T.; Bayón, R. Enhanced Tribological Performance of Cylinder Liners Made of Cast Aluminum Alloy with High Silicon Content through Plasma Electrolytic Oxidation. *Surf. Coat. Technol.* **2022**, *433*, 128146. [[CrossRef](#)]
24. Abdulwahab, A.; Shrestha, S.; Brooks, P.; Barton, D. *Thermal Performance of PEO Coated Lightweight Brake Rotors Compared With Grey Cast Iron*; International Federation of Automotive Engineering Societies (FISITA): Maastricht, The Netherlands, 2014; pp. 13–15.
25. Li, K.; Zhang, G.; Yi, A.; Zhu, W.; Liao, Z.; Chen, K.; Li, W.; Luo, Z. Effects of Matrix Silicon Content on the Plasma Electrolytic Oxidation of Al-Si Alloys Using Different Power Modes. *Crystals* **2022**, *12*, 123. [[CrossRef](#)]
26. Shakil, S.I.; Hadadzadeh, A.; Shalchi Amirkhiz, B.; Pirgazi, H.; Mohammadi, M.; Haghshenas, M. Additive Manufactured versus Cast AlSi10Mg Alloy: Microstructure and Micromechanics. *Results Mater.* **2021**, *10*, 100178. [[CrossRef](#)]
27. Yu, H.; Dong, Q.; Chen, Y.; Chen, C. Influence of Silicon on Growth Mechanism of Micro-Arc Oxidation Coating on Cast Al-Si Alloy. *R. Soc. Open Sci.* **2018**, *5*, 172428. [[CrossRef](#)] [[PubMed](#)]
28. Rogov, A.B.; Lyu, H.; Matthews, A.; Yerokhin, A. AC Plasma Electrolytic Oxidation of Additively Manufactured and Cast AlSi12 Alloys. *Surf. Coat. Technol.* **2020**, *399*, 126116. [[CrossRef](#)]
29. Sabatini, G.; Ceschini, L.; Martini, C.; Williams, J.A.; Hutchings, I.M. Improving Sliding and Abrasive Wear Behaviour of Cast A356 and Wrought AA7075 Aluminium Alloys by Plasma Electrolytic Oxidation. *Mater. Des.* **2010**, *31*, 816–828. [[CrossRef](#)]
30. Yoshida, H.; Uchida, H. Heat Treatment of Aluminum Alloys. *Keikinzoku/J. Jpn. Inst. Light Met.* **1995**, *45*, 41–55. [[CrossRef](#)]
31. Mohedano, M.; Matykina, E.; Arrabal, R.; Mingo, B.; Pardo, A. PEO of Pre-Anodized Al-Si Alloys: Corrosion Properties and Influence of Sealings. *Appl. Surf. Sci.* **2015**, *346*, 57–67. [[CrossRef](#)]
32. Liang, Z.X.; Ye, B.; Zhang, L.; Wang, Q.G.; Yang, W.Y.; Wang, Q.D. A New High-Strength and Corrosion-Resistant Al-Si Based Casting Alloy. *Mater. Lett.* **2013**, *97*, 104–107. [[CrossRef](#)]
33. Yerokhin, A.; Khan, R.H.U. Anodising of Light Alloys. *Surf. Eng. Light Alloy. Alum. Magnes. Titan. Alloy.* **2010**, 83–109. [[CrossRef](#)]
34. He, J.; Cai, Q.Z.; Luo, H.H.; Yu, L.; Wei, B.K. Influence of Silicon on Growth Process of Plasma Electrolytic Oxidation Coating on Al-Si Alloy. *J. Alloys Compd.* **2009**, *471*, 395–399. [[CrossRef](#)]
35. Nagumothu, R.B.; Thangavelu, A.; Nair, A.M.; Sukumaran, A.; Anjilivelil, T. Development of Black Corrosion-Resistant Ceramic Oxide Coatings on AA7075 by Plasma Electrolytic Oxidation. *Trans. Indian Inst. Met.* **2019**, *72*, 47–53. [[CrossRef](#)]
36. Akbar, A.; Adnan Qaiser, M.; Hussain, A.; Ali Mustafa, R.; Xiong, D.; Adnan Akbar, E. Surface Modification of Aluminum Alloy 6060 through Plasma Electrolytic Oxidation. *Int. J. Eng. Work. Kambohwell Publ. Enterp.* **2017**, *4*, 114–123.
37. Jiang, B.L.; Wang, Y.M. Plasma Electrolytic Oxidation Treatment of Aluminium and Titanium Alloys. *Surf. Eng. Light Alloy. Alum. Magnes. Titan. Alloy.* **2010**, 110–154. [[CrossRef](#)]
38. Aliofkhaezrai, M.; Macdonald, D.D.; Matykina, E.; Parfenov, E.V.; Egorkin, V.S.; Curran, J.A.; Troughton, S.C.; Sinebryukhov, S.L.; Gnednikov, S.V.; Lampke, T.; et al. Review of Plasma Electrolytic Oxidation of Titanium Substrates: Mechanism, Properties, Applications and Limitations. *Appl. Surf. Sci. Adv.* **2021**, *5*, 100121. [[CrossRef](#)]
39. Fattah-alhosseini, A.; Chaharmahali, R.; Babaei, K. Effect of Particles Addition to Solution of Plasma Electrolytic Oxidation (PEO) on the Properties of PEO Coatings Formed on Magnesium and Its Alloys: A Review. *J. Magnes. Alloy.* **2020**, *8*, 799–818. [[CrossRef](#)]

40. Guo, Y.; Rogov, A.; Hird, A.; Mingo, B.; Matthews, A.; Yerokhin, A. Plasma Electrolytic Oxidation of Magnesium by Sawtooth Pulse Current. *Surf. Coat. Technol.* **2022**, *429*, 127938. [[CrossRef](#)]
41. Apelfeld, A.V.; Betsofen, S.Y.; Borisov, A.M.; Vladimirov, B.V.; Savushkina, S.V.; Knyazev, E.V. Stabilization of the High-Temperature Phases in Ceramic Coatings on Zirconium Alloy Produced by Plasma Electrolytic Oxidation. *J. Phys. Conf. Ser.* **2016**, *748*, 2–7. [[CrossRef](#)]
42. Babaei, K.; Fattah-alhosseini, A.; Chaharmahali, R. A Review on Plasma Electrolytic Oxidation (PEO) of Niobium: Mechanism, Properties and Applications. *Surf. Interfaces* **2020**, *21*, 100719. [[CrossRef](#)]
43. Antonio, R.F.; Rangel, E.C.; Mas, B.A.; Duek, E.A.R.; Cruz, N.C. Growth of Hydroxyapatite Coatings on Tantalum by Plasma Electrolytic Oxidation in a Single Step. *Surf. Coat. Technol.* **2019**, *357*, 698–705. [[CrossRef](#)]
44. Wang, Y.; Jiang, Z.; Yao, Z. Effects of Na₂WO₄ and Na₂SiO₃ Additives in Electrolytes on Microstructure and Properties of PEO Coatings on Q235 Carbon Steel. *J. Alloys Compd.* **2009**, *481*, 725–729. [[CrossRef](#)]
45. Wang, Y.; Jiang, Z.; Yao, Z. Preparation and Properties of Ceramic Coating on Q235 Carbon Steel by Plasma Electrolytic Oxidation. *Curr. Appl. Phys.* **2009**, *9*, 1067–1071. [[CrossRef](#)]
46. Malinovski, V.; Marin, A.; Mihalache, M.; Iosub, I. Preparation and Characterization of Coatings on Carbon Steel Obtained by PEO in Silicate/Carbonate Electrolyte. *Surf. Coat. Technol.* **2016**, *296*, 96–103. [[CrossRef](#)]
47. Wu, T.; Blawert, C.; Zheludkevich, M.L. Influence of Secondary Phases of AlSi₉Cu₃ Alloy on the Plasma Electrolytic Oxidation Coating Formation Process. *J. Mater. Sci. Technol.* **2020**, *50*, 75–85. [[CrossRef](#)]
48. Pezzato, L.; Brunelli, K.; Dabalà, M. Corrosion Properties of Plasma Electrolytic Oxidation Coated AA7075 Treated Using an Electrolyte Containing Lanthanum-Salts. *Surf. Interface Anal.* **2016**, *48*, 729–738. [[CrossRef](#)]
49. Martin, J.; Melhem, A.; Shchedrina, I.; Duchanoy, T.; Nominé, A.; Henrion, G.; Czerwiec, T.; Belmonte, T. Effects of Electrical Parameters on Plasma Electrolytic Oxidation of Aluminium. *Surf. Coat. Technol.* **2013**, *221*, 70–76. [[CrossRef](#)]
50. An, L.Y.; Ying, M.A.; Yan, X.X.; Sheng WA, N.G.; Wang, Z.Y. Effects of Electrical Parameters and Their Interactions on Plasma Electrolytic Oxidation Coatings on Aluminum Substrates. *Trans. Nonferrous Met. Soc. China (Engl. Ed.)* **2020**, *30*, 883–895. [[CrossRef](#)]
51. Dehnavi, V.; Liu, X.Y.; Luan, B.L.; Shoosmith, D.W.; Rohani, S. Phase Transformation in Plasma Electrolytic Oxidation Coatings on 6061 Aluminum Alloy. *Surf. Coat. Technol.* **2014**, *251*, 106–114. [[CrossRef](#)]
52. Sieber, M.; Simchen, F.; Morgenstern, R.; Scharf, I.; Lampke, T. Plasma Electrolytic Oxidation of High-Strength Aluminium Alloys—Substrate Effect on Wear and Corrosion Performance. *Metals* **2018**, *8*, 356. [[CrossRef](#)]
53. del Olmo, R.; Mohedano, M.; Visser, P.; Matykina, E.; Arrabal, R. Flash-PEO Coatings Loaded with Corrosion Inhibitors on AA2024. *Surf. Coat. Technol.* **2020**, *402*, 126317. [[CrossRef](#)]
54. Xie, H.J.; Cheng, Y.L.; Li, S.X.; Cao, J.H.; Li, C.A.O. Wear and Corrosion Resistant Coatings on Surface of Cast A356 Aluminum Alloy by Plasma Electrolytic Oxidation in Moderately Concentrated Aluminate Electrolytes. *Trans. Nonferrous Met. Soc. China (Engl. Ed.)* **2017**, *27*, 336–351. [[CrossRef](#)]
55. Shirani, A.; Joy, T.; Rogov, A.; Lin, M.; Yerokhin, A.; Mogonye, J.E.; Korenyi-Both, A.; Aouadi, S.M.; Voevodin, A.A.; Berman, D. PEO-Chameleon as a Potential Protective Coating on Cast Aluminum Alloys for High-Temperature Applications. *Surf. Coatings Technol.* **2020**, *397*, 126016. [[CrossRef](#)]
56. Wang, R. High Current Plasma Electrolytic Oxidation Coating Processes for Wear and Corrosion Prevention of Al 2024. *Electron. Theses Diss.* **2018**, *116*, 7405.
57. Clyne, T.W.; Troughton, S.C. A Review of Recent Work on Discharge Characteristics during Plasma Electrolytic Oxidation of Various Metals. *Int. Mater. Rev.* **2019**, *64*, 127–162. [[CrossRef](#)]
58. Pezzato, L.; Rigon, M.; Martucci, A.; Brunelli, K.; Dabalà, M. Plasma Electrolytic Oxidation (PEO) as Pre-Treatment for Sol-Gel Coating on Aluminum and Magnesium Alloys. *Surf. Coat. Technol.* **2019**, *366*, 114–123. [[CrossRef](#)]
59. Li, T.; Li, L.; Qi, J.; Chen, F. Corrosion Protection of Ti6Al4V by a Composite Coating with a Plasma Electrolytic Oxidation Layer and Sol-Gel Layer Filled with Graphene Oxide. *Prog. Org. Coat.* **2020**, *144*. [[CrossRef](#)]
60. Phuong, N.V.; Fazal, B.R.; Moon, S. Cerium- and Phosphate-Based Sealing Treatments of PEO Coated AZ31 Mg Alloy. *Surf. Coat. Technol.* **2017**, *309*, 86–95. [[CrossRef](#)]
61. Curran, J.A.; Kalkanci, H.; Magurova, Y.; Clyne, T.W. Mullite-Rich Plasma Electrolytic Oxide Coatings for Thermal Barrier Applications. *Surf. Coat. Technol.* **2007**, *201*, 8683–8687. [[CrossRef](#)]
62. Wang, P.; Li, J.; Guo, Y.; Wang, J.; Yang, Z.; Liang, M. Effect of Zirconia Sol on the Microstructures and Thermal-Protective Properties of PEO Coating on a Cast Al-12Si Piston Alloy. *J. Alloys Compd.* **2016**, *657*, 703–710. [[CrossRef](#)]
63. Dou, B.; Wang, Y.; Zhang, T.; Liu, B.; Shao, Y.; Meng, G.; Wang, F. Growth Behaviors of Layered Double Hydroxide on Microarc Oxidation Film and Anti-Corrosion Performances of the Composite Film. *J. Electrochem. Soc.* **2016**, *163*, C917–C927. [[CrossRef](#)]
64. Lee, J.H.; Jung, K.H.; Kim, S.J. Characterization of Ceramic Oxide Coatings Prepared by Plasma Electrolytic Oxidation Using Pulsed Direct Current with Different Duty Ratio and Frequency. *Appl. Surf. Sci.* **2020**, *516*, 146049. [[CrossRef](#)]
65. Stojadinović, S.; Radić, N.; Grbić, B.; Maletić, S.; Stefanov, P.; Pačevski, A.; Vasilić, R. Structural, Photoluminescent and Photocatalytic Properties of TiO₂: Eu³⁺ Coatings Formed by Plasma Electrolytic Oxidation. *Appl. Surf. Sci.* **2016**, *370*, 218–228. [[CrossRef](#)]
66. Tadić, N.; Stojadinović, S.; Radić, N.; Grbić, B.; Vasilić, R. Characterization and Photocatalytic Properties of Tungsten Doped TiO₂ Coatings on Aluminum Obtained by Plasma Electrolytic Oxidation. *Surf. Coat. Technol.* **2016**, *305*, 192–199. [[CrossRef](#)]

67. Chen, Z.; Yan, X.; Chang, Y.; Xie, S.; Ma, W.; Zhao, G.; Liao, H.; Fang, H.; Liu, M.; Cai, D. Effect of Polarization Voltage on the Surface Componentization and Biocompatibility of Micro-Arc Oxidation Modified Selective Laser Melted Ti6Al4V. *Mater. Res. Express* **2019**, *6*, 086425. [[CrossRef](#)]
68. Yeung, W.K.; Sukhorukova, I.V.; Shtansky, D.V.; Levashov, E.A.; Zhitnyak, I.Y.; Gloushankova, N.A.; Kiryukhantsev-Korneev, P.V.; Petrzhik, M.I.; Matthews, A.; Yerokhin, A. Characteristics and in Vitro Response of Thin Hydroxyapatite-Titania Films Produced by Plasma Electrolytic Oxidation of Ti Alloys in Electrolytes with Particle Additions. *RSC Adv.* **2016**, *6*, 12688–12698. [[CrossRef](#)] [[PubMed](#)]
69. Fattah-alhosseini, A.; Molaei, M.; Nouri, M.; Babaei, K. Antibacterial Activity of Bioceramic Coatings on Mg and Its Alloys Created by Plasma Electrolytic Oxidation (PEO): A Review. *J. Magnes. Alloy.* **2022**, *10*, 81–96. [[CrossRef](#)]
70. Gnedenkov, S.V.; Sinebryukhov, S.L.; Zavidnaya, A.G.; Egorkin, V.S.; Puz', A.V.; Mashtalyar, D.V.; Sergienko, V.I.; Yerokhin, A.L.; Matthews, A. Composite Hydroxyapatite-PTFE Coatings on Mg-Mn-Ce Alloy for Resorbable Implant Applications via a Plasma Electrolytic Oxidation-Based Route. *J. Taiwan Inst. Chem. Eng.* **2014**, *45*, 3104–3109. [[CrossRef](#)]
71. Cordeiro, J.M.; Nagay, B.E.; Ribeiro, A.L.R.; da Cruz, N.C.; Rangel, E.C.; Fais, L.M.G.; Vaz, L.G.; Barão, V.A.R. Functionalization of an Experimental Ti-Nb-Zr-Ta Alloy with a Biomimetic Coating Produced by Plasma Electrolytic Oxidation. *J. Alloys Compd.* **2019**, *770*, 1038–1048. [[CrossRef](#)]
72. Sluginov, N.P. On Luminous Phenomen, Observed in Liquids during Electrolysis. *Russ. Phys. Chem. Soc* **1880**, *12*, 193–203.
73. Snezhko, L.A.; Beskrovnyi, I.M.; Nevkrytyi, V.I.; Chernenko, V.I. Impulsnyi Rezhim Dlia Poluchenii Silikatnykh Pokrytii v Iskrovom Razriade. *Zashch. Met.* **1980**, *16*, 365.
74. Markov, G.A.; Mironova, M.K.; Potapova, O.G.; Tatarchuk, O.A. Structure of Anodic Films Obtained by Micro Arc Oxidation of Aluminum. *Izv. Akad. Nauk SSSR Neorg. Mater.* **1983**, *19*, 1110–1113.
75. Malyshev, V.N.; Bulychev, S.I.; Markov, G.A. Physical and Mechanical Characteristics and Wear Resistance of Coatings Formed by Microarc Oxidation Method, *Physika i Khimija Obrab. Fiz. Khim. Obrab. Mater.* **1985**, *1*, 82–87.
76. Dittrich, K.-H.; Krysmann, W.; Kurze, P.; Scheneider, H.G. Structure and Properties of ANOF Layers. *Cryst. Res. Technol.* **1984**, *19*, 93–99. [[CrossRef](#)]
77. Krysmann, W.; Kurze, P.; Dittrich, K.-H.; Schneider, H.G. Process Characteristics and Parameters of Anodic Oxidation by Spark Discharge (ANOF). *Cryst. Res. Technol.* **1984**, *19*, 973–979. [[CrossRef](#)]
78. Yerokhin, A.L.; Voevodin, A.A.; Lyubimov, V.V.; Zabinski, J.; Donley, M. Plasma Electrolytic Fabrication of Oxide Ceramic Surface Layers for Tribotechnical Purposes on Aluminium Alloys. *Surf. Coatings Technol.* **1998**, *110*, 140–146. [[CrossRef](#)]
79. Yerokhin, A.L.; Nie, X.; Leyland, A.; Matthews, A.; Dowey, S.J. Plasma Electrolysis for Surface Engineering. *Surf. Coatings Technol.* **1999**, *122*, 73–93. [[CrossRef](#)]
80. Dehnavi, V.; Luan, B.L.; Shoesmith, D.W.; Liu, X.Y.; Rohani, S. Effect of Duty Cycle and Applied Current Frequency on Plasma Electrolytic Oxidation (PEO) Coating Growth Behavior. *Surf. Coatings Technol.* **2013**, *226*, 100–107. [[CrossRef](#)]
81. Chaharmahali, R.; Fattah-alhosseini, A.; Babaei, K. Surface Characterization and Corrosion Behavior of Calcium Phosphate (Ca-P) Base Composite Layer on Mg and Its Alloys Using Plasma Electrolytic Oxidation (PEO): A Review. *J. Magnes. Alloy.* **2021**, *9*, 21–40. [[CrossRef](#)]
82. Tang, M.; Li, W.; Liu, H.; Zhu, L. Influence of K₂TiF₆ in Electrolyte on Characteristics of the Microarc Oxidation Coating on Aluminum Alloy. *Curr. Appl. Phys.* **2012**, *12*, 1259–1265. [[CrossRef](#)]
83. Simchen, F.; Sieber, M.; Lampke, T. Electrolyte Influence on Ignition of Plasma Electrolytic Oxidation Processes on Light Metals. *Surf. Coatings Technol.* **2017**, *315*, 205–213. [[CrossRef](#)]
84. Zhang, P.; Nie, X.; Hu, H.; Liu, Y. TEM Analysis and Tribological Properties of Plasma Electrolytic Oxidation (PEO) Coatings on a Magnesium Engine AJ62 Alloy. *Surf. Coatings Technol.* **2010**, *205*, 1508–1514. [[CrossRef](#)]
85. Pan, J.; Wen, Y.; Wang, L.; Wu, Z.; Dong, H.; Ye, Z. Doping and Defects: The Coloring Mechanism of Black Plasma Electrolytic Oxidation (PEO) Films on Aluminum Alloys. *Surf. Coatings Technol.* **2022**, *431*, 128035. [[CrossRef](#)]
86. Arunnellaiappan, T.; Rama Krishna, L.; Anoop, S.; Uma Rani, R.; Rameshbabu, N. Fabrication of Multifunctional Black PEO Coatings on AA7075 for Spacecraft Applications. *Surf. Coatings Technol.* **2016**, *307*, 735–746. [[CrossRef](#)]
87. Rogov, A.B.; Huang, Y.; Shore, D.; Matthews, A.; Yerokhin, A. Toward Rational Design of Ceramic Coatings Generated on Valve Metals by Plasma Electrolytic Oxidation: The Role of Cathodic Polarisation. *Ceram. Int.* **2021**, *47*, 34137–34158. [[CrossRef](#)]
88. Tsai, D.S.; Chou, C.C. Review of the Soft Sparking Issues in Plasma Electrolytic Oxidation. *Metals* **2018**, *8*, 105. [[CrossRef](#)]
89. Gao, Y.; Yerokhin, A.; Matthews, A. Effect of Current Mode on PEO Treatment of Magnesium in Ca- and P-Containing Electrolyte and Resulting Coatings. *Appl. Surf. Sci.* **2014**, *316*, 558–567. [[CrossRef](#)]
90. Kaseem, M.; Yang, H.W.; Ko, Y.G. Toward a Nearly Defect-Free Coating via High-Energy Plasma Sparks. *Sci. Rep.* **2017**, *7*, 2378. [[CrossRef](#)]
91. Rogov, A.B.; Matthews, A.; Yerokhin, A. Role of Cathodic Current in Plasma Electrolytic Oxidation of Al: A Quantitative Approach to in-Situ Evaluation of Cathodically Induced Effects. *Electrochim. Acta* **2019**, *317*, 221–231. [[CrossRef](#)]
92. Mohedano, M.; Arrabal, R.; Mingo, B.; Pardo, A.; Matykina, E. Role of Particle Type and Concentration on Characteristics of PEO Coatings on AM50 Magnesium Alloy. *Surf. Coatings Technol.* **2018**, *334*, 328–335. [[CrossRef](#)]
93. Aliasghari, S.; Rogov, A.; Skeldon, P.; Zhou, X.; Yerokhin, A.; Aliabadi, A.; Ghorbani, M. Plasma Electrolytic Oxidation and Corrosion Protection of Friction Stir Welded AZ31B Magnesium Alloy-Titanium Joints. *Surf. Coatings Technol.* **2020**, *393*, 125838. [[CrossRef](#)]

94. Urban, M. Plasma Electrolytic Oxidation of Magnesium Alloys for Automotive Applications. Ph.D. Thesis, The University of Manchester, Manchester, UK, 2014; p. 116.
95. Hussein, R.O.; Nie, X.; Northwood, D.O. An Investigation of Ceramic Coating Growth Mechanisms in Plasma Electrolytic Oxidation (PEO) Processing. *Electrochim. Acta* **2013**, *112*, 111–119. [[CrossRef](#)]
96. Li, Q.; Liang, J.; Wang, Q. Plasma Electrolytic Oxidation Coatings on Lightweight Metals. *Mod. Surf. Eng. Treat.* **2013**. [[CrossRef](#)]
97. Zhu, Z.; Tu, W.; Cheng, Y.; Cheng, Y. The Formation of Metallic W and Amorphous Phase in the Plasma Electrolytic Oxidation Coatings on an Al Alloy from Tungstate-Containing Electrolyte. *Surf. Coatings Technol.* **2019**, *361*, 176–187. [[CrossRef](#)]
98. Hakimzad, A.; Raeissi, K.; Golozar, M.A.; Lu, X.; Blawert, C.; Zheludkevich, M.L. The Effect of Pulse Waveforms on Surface Morphology, Composition and Corrosion Behavior of Al₂O₃ and Al₂O₃/TiO₂ Nano-Composite PEO Coatings on 7075 Aluminum Alloy. *Surf. Coatings Technol.* **2017**, *324*, 208–221. [[CrossRef](#)]
99. Lonyuk, B.; Apachitei, I.; Duszczyc, J. The Effect of Oxide Coatings on Fatigue Properties of 7475-T6 Aluminium Alloy. *Surf. Coatings Technol.* **2007**, *201*, 8688–8694. [[CrossRef](#)]
100. Kaseem, M.; Fatimah, S.; Nashrah, N.; Ko, Y.G. Recent Progress in Surface Modification of Metals Coated by Plasma Electrolytic Oxidation: Principle, Structure, and Performance. *Prog. Mater. Sci.* **2021**, *117*, 100735. [[CrossRef](#)]
101. Toulabifard, A.; Rahmati, M.; Raeissi, K.; Hakimzad, A.; Santamaria, M. The Effect of Electrolytic Solution Composition on the Structure, Corrosion, and Wear Resistance of PEO Coatings on AZ31 Magnesium Alloy. *Coatings* **2020**, *10*, 937. [[CrossRef](#)]
102. Zhu, L.; Guo, Z.; Zhang, Y.; Li, Z.; Sui, M. A Mechanism for the Growth of a Plasma Electrolytic Oxide Coating on Al. *Electrochim. Acta* **2016**, *208*, 296–303. [[CrossRef](#)]
103. Blawert, C.; Sah, S.P.; Liang, J.; Huang, Y.; Höche, D. Role of Sintering and Clay Particle Additions on Coating Formation during PEO Processing of AM50 Magnesium Alloy. *Surf. Coatings Technol.* **2012**, *213*, 48–58. [[CrossRef](#)]
104. Vijh, K. Sparking Voltages and Side Reactions during Anodization of Valve Metals in Terms of Electron Tunneling. *Corros. Sci.* **1971**, *1*, 411–417. [[CrossRef](#)]
105. Ikonopisov, S. Theory of Electrical Breakdown during Formation of Barrier Anodic Films. *Electrochim. Acta* **1977**, *22*, 1077–1082. [[CrossRef](#)]
106. Albella, J.M.; Montero, I.; Martínez-Duart, J.M. Electron Injection and Avalanche during the Anodic Oxidation of Tantalum. *J. Electrochem. Soc.* **1984**, *131*, 1101–1104. [[CrossRef](#)]
107. Albella, J.M.; Montero, I.; Martínez-Duart, J.M. A Theory of Avalanche Breakdown during Anodic Oxidation. *Electrochim. Acta* **1987**, *32*, 255–258. [[CrossRef](#)]
108. Ingenieurwissenschaften, D. Der Simulation of Plasma Electrolytic Oxidation (PEO) of AM50 Mg Alloys and Its Experimental Validation. *Dissertation* **2018**, 154.
109. Wang, L.; Chen, L.; Yan, Z.; Fu, W. Optical Emission Spectroscopy Studies of Discharge Mechanism and Plasma Characteristics during Plasma Electrolytic Oxidation of Magnesium in Different Electrolytes. *Surf. Coatings Technol.* **2010**, *205*, 1651–1658. [[CrossRef](#)]
110. Xue, W.; Deng, Z.; Chen, R.; Zhang, T. Growth Regularity of Ceramic Coatings Formed by Microarc Oxidation on Al-Cu-Mg Alloy. *Thin Solid Films* **2000**, *372*, 114–117. [[CrossRef](#)]
111. Molak, R.M.; Topolski, K.; Szychalski, M.; Dulińska-Molak, I.; Morończyk, B.; Pakieła, Z.; Nieużyła, L.; Mazurkiewicz, M.; Wojucki, M.; Gebeshuber, A.; et al. Functional Properties of the Novel Hybrid Coatings Combined of the Oxide and DLC Layer as a Protective Coating for AZ91E Magnesium Alloy. *Surf. Coatings Technol.* **2019**, *380*, 125040. [[CrossRef](#)]
112. Yaakop, N. *Plasma Electrolytic Oxidation of Aluminium for Power Electronics Applications*; The University of Manchester: Manchester, UK, 2018.
113. Monfort, F.; Matykina, E.; Berkani, A.; Skeldon, P.; Thompson, G.E.; Habazaki, H.; Shimizu, K. Species Separation during Coating Growth on Aluminium by Spark Anodizing. *Surf. Coatings Technol.* **2007**, *201*, 8671–8676. [[CrossRef](#)]
114. Wang, R.; Wu, Y.; Wu, G.; Chen, D.; He, D.; Li, D.; Guo, C.; Zhou, Y.; Shen, D.; Nash, P. An Investigation about the Evolution of Microstructure and Composition Difference between Two Interfaces of Plasma Electrolytic Oxidation Coatings on Al. *J. Alloys Compd.* **2018**, *753*, 272–281. [[CrossRef](#)]
115. Wang, D.D.; Liu, X.T.; Wu, Y.K.; Han, H.P.; Yang, Z.; Su, Y.; Zhang, X.Z.; Wu, G.R.; Shen, D.J. Evolution Process of the Plasma Electrolytic Oxidation (PEO) Coating Formed on Aluminum in an Alkaline Sodium Hexametaphosphate ((NaPO₃)₆) Electrolyte. *J. Alloys Compd.* **2019**, *798*, 129–143. [[CrossRef](#)]
116. Huang, X. Plasma Electrolytic Oxidation Coatings on Aluminum Alloys: Microstructures, Properties, and Applications. *Mod. Concepts Mater. Sci.* **2019**, *2*, 000526. [[CrossRef](#)]
117. Zhu, L.; Ke, X.; Li, J.; Zhang, Y.; Zhang, Z.; Sui, M. Growth Mechanisms for Initial Stages of Plasma Electrolytic Oxidation Coating on Al. *Surf. Interfaces* **2021**, *25*, 101186. [[CrossRef](#)]
118. Barati, N.; Jiang, J.; Meletis, E.I. Microstructural Evolution of Ceramic Nanocomposites Coated on 7075 Al Alloy by Plasma Electrolytic Oxidation. *Surf. Coatings Technol.* **2022**, *437*, 128345. [[CrossRef](#)]
119. Rogov, A.B.; Nemcova, A.; Hashimoto, T.; Matthews, A.; Yerokhin, A. Analysis of Electrical Response, Gas Evolution and Coating Morphology during Transition to Soft Sparking PEO of Al. *Surf. Coatings Technol.* **2022**, 128142. [[CrossRef](#)]
120. Rogov, A.B.; Yerokhin, A.; Matthews, A. The Role of Cathodic Current in Plasma Electrolytic Oxidation of Aluminum: Phenomenological Concepts of the “Soft Sparking” Mode. *Langmuir* **2017**, *33*, 11059–11069. [[CrossRef](#)] [[PubMed](#)]

121. Mohedano, M.; Matykina, E.; Arrabal, R.; Mingo, B.; Zheludkevich, M.L. PEO of Rheocast A356 Al Alloy: Energy Efficiency and Corrosion Properties. *Surf. Interface Anal.* **2016**, *48*, 953–959. [[CrossRef](#)]
122. Martin, J.; Leone, P.; Nominé, A.; Veys-Renaux, D.; Henrion, G.; Belmonte, T. Influence of Electrolyte Ageing on the Plasma Electrolytic Oxidation of Aluminium. *Surf. Coatings Technol.* **2015**, *269*, 36–46. [[CrossRef](#)]
123. Guan, Y.J.; Xia, Y.; Li, G. Growth Mechanism and Corrosion Behavior of Ceramic Coatings on Aluminum Produced by Autocontrol AC Pulse PEO. *Surf. Coatings Technol.* **2008**, *202*, 4602–4612. [[CrossRef](#)]
124. Nie, X.; Meletis, E.I.; Jiang, J.C.; Leyland, A.; Yerokhin, A.L.; Matthews, A. Abrasive Wear/Corrosion Properties and TEM Analysis of Al₂O₃ Coatings Fabricated Using Plasma Electrolysis. *Surf. Coatings Technol.* **2002**, *149*, 245–251. [[CrossRef](#)]
125. Cheng, Y.L.; Xie, H.J.; Cao, J.H.; Cheng, Y.L. Effect of NaOH on Plasma Electrolytic Oxidation of A356 Aluminium Alloy in Moderately Concentrated Aluminate Electrolyte. *Trans. Nonferrous Met. Soc. China (English Ed.)* **2021**, *31*, 3677–3690. [[CrossRef](#)]
126. Wang, L.; Wang, G.; Dong, H.; Ye, M.; Li, X.; Liu, L.; Pan, J.; Ye, Z. Plasma Electrolytic Oxidation Coatings on Additively Manufactured Aluminum–Silicon Alloys with Superior Tribological Performance. *Surf. Coatings Technol.* **2022**, *435*, 128246. [[CrossRef](#)]
127. Oh, Y.J.; Mun, J.I.; Kim, J.H. Effects of Alloying Elements on Microstructure and Protective Properties of Al₂O₃ Coatings Formed on Aluminum Alloy Substrates by Plasma Electrolysis. *Surf. Coatings Technol.* **2009**, *204*, 141–148. [[CrossRef](#)]
128. Cheng, Y.L.; Mao, M.K.; Cao, J.H.; Peng, Z.M. Plasma Electrolytic Oxidation of an Al-Cu-Li Alloy in Alkaline Aluminate Electrolytes: A Competition between Growth and Dissolution for the Initial Ultra-Thin Films. *Electrochim. Acta* **2014**, *138*, 417–429. [[CrossRef](#)]
129. Xu, F.; Xia, Y.; Li, G. The Mechanism of PEO Process on Al-Si Alloys with the Bulk Primary Silicon. *Appl. Surf. Sci.* **2009**, *255*, 9531–9538. [[CrossRef](#)]
130. Khan, R.H.U.; Yerokhin, A.; Li, X.; Dong, H.; Matthews, A. Surface Characterisation of DC Plasma Electrolytic Oxidation Treated 6082 Aluminium Alloy: Effect of Current Density and Electrolyte Concentration. *Surf. Coatings Technol.* **2010**, *205*, 1679–1688. [[CrossRef](#)]
131. Rogov, A.B.; Yerokhin, A.; Matthews, A. The Role of Cathodic Current in Plasma Electrolytic Oxidation of Aluminium: Current Density “scanning Waves” on Complex-Shape Substrates. *J. Phys. D Appl. Phys.* **2018**, *51*, 405303. [[CrossRef](#)]
132. Matykina, E.; Arrabal, R.; Mohedano, M.; Mingo, B.; Gonzalez, J.; Pardo, A.; Merino, M.C. Recent Advances in Energy Efficient PEO Processing of Aluminium Alloys. *Trans. Nonferrous Met. Soc. China (English Ed.)* **2017**, *27*, 1439–1454. [[CrossRef](#)]
133. Liu, S.; Zeng, J. Effects of Negative Voltage on Microstructure and Corrosion Resistance of Red Mud Plasma Electrolytic Oxidation Coatings. *Surf. Coatings Technol.* **2018**, *352*, 15–25. [[CrossRef](#)]
134. Molaei, M.; Fattah-alhosseini, A.; Nouri, M.; Nourian, A. Systematic Optimization of Corrosion, Bioactivity, and Biocompatibility Behaviors of Calcium-Phosphate Plasma Electrolytic Oxidation (PEO) Coatings on Titanium Substrates. *Ceram. Int.* **2022**, *48*, 6322–6337. [[CrossRef](#)]
135. Wang, S.; Liu, X.; Yin, X.; Du, N. Influence of Electrolyte Components on the Microstructure and Growth Mechanism of Plasma Electrolytic Oxidation Coatings on 1060 Aluminum Alloy. *Surf. Coatings Technol.* **2020**, *381*, 125214. [[CrossRef](#)]
136. Cheng, Y.; Cao, J.; Mao, M.; Peng, Z.; Skeldon, P.; Thompson, G.E. High Growth Rate, Wear Resistant Coatings on an Al-Cu-Li Alloy by Plasma Electrolytic Oxidation in Concentrated Aluminate Electrolytes. *Surf. Coatings Technol.* **2015**, *269*, 74–82. [[CrossRef](#)]
137. Sharma, A.; Jang, Y.J.; Jung, J.P. Effect of KOH to Na₂SiO₃ Ratio on Microstructure and Hardness of Plasma Electrolytic Oxidation Coatings on AA 6061 Alloy. *J. Mater. Eng. Perform.* **2017**, *26*, 5032–5042. [[CrossRef](#)]
138. Yang, Z.; Zhang, X.Z.; Wu, Y.K.; Wu, G.R.; Wang, D.D.; Liu, X.T.; Han, H.P.; Su, Y.; Shen, D.J. The Correlation between the Na₂SiO₃·9H₂O Concentrations and the Characteristics of Plasma Electrolytic Oxidation Ceramic Coatings. *Ceram. Int.* **2019**, *45*, 19388–19394. [[CrossRef](#)]
139. Sundararajan, G.; Rama Krishna, L. Mechanisms Underlying the Formation of Thick Alumina Coatings through the MAO Coating Technology. *Surf. Coatings Technol.* **2003**, *167*, 269–277. [[CrossRef](#)]
140. Lv, G.; Gu, W.; Chen, H.; Feng, W.; Khosa, M.L.; Li, L.; Niu, E.; Zhang, G.; Yang, S.-Z. Characteristic of Ceramic Coatings on Aluminum by Plasma Electrolytic Oxidation in Silicate and Phosphate Electrolyte. *Appl. Surf. Sci.* **2006**, *253*, 2947–2952. [[CrossRef](#)]
141. Erfanifar, E.; Aliofkhaezrai, M.; Fakhr Nabavi, H.; Sharifi, H.; Rouhaghdam, A.S. Growth Kinetics and Morphology of Plasma Electrolytic Oxidation Coating on Aluminum. *Mater. Chem. Phys.* **2017**, *185*, 162–175. [[CrossRef](#)]
142. Sabouri, M.; Mousavi Khoei, S.M. Plasma Electrolytic Oxidation in the Presence of Multiwall Carbon Nanotubes on Aluminum Substrate: Morphological and Corrosion Studies. *Surf. Coatings Technol.* **2018**, *334*, 543–555. [[CrossRef](#)]
143. Salehi Doolabi, D.; Ehteshamzadeh, M.; Mirhosseini, S.M.M. Effect of NaOH on the Structure and Corrosion Performance of Alumina and Silica PEO Coatings on Aluminum. *J. Mater. Eng. Perform.* **2012**, *21*, 2195–2202. [[CrossRef](#)]
144. del Olmo, R.; Mohedano, M.; Mingo, B.; Arrabal, R.; Matykina, E. LDH Post-Treatment of Flash PEO Coatings. *Coatings* **2019**, *9*, 6–20. [[CrossRef](#)]
145. Walsh, F.C.; Low, C.T.J.; Wood, R.J.K.; Stevens, K.T.; Archer, J.; Poeton, A.R.; Ryder, A. Plasma Electrolytic Oxidation (PEO) for Production of Anodised Coatings on Lightweight Metal (Al, Mg, Ti) Alloys. *Trans. Inst. Met. Finish.* **2009**, *87*, 122–135. [[CrossRef](#)]
146. Habazaki, H.; Tsunekawa, S.; Tsuji, E.; Nakayama, T. Formation and Characterization of Wear-Resistant PEO Coatings Formed on β-Titanium Alloy at Different Electrolyte Temperatures. *Appl. Surf. Sci.* **2012**, *259*, 711–718. [[CrossRef](#)]
147. Al Afghani, F.; Anawati, A. Plasma Electrolytic Oxidation of Zircaloy-4 in a Mixed Alkaline Electrolyte. *Surf. Coatings Technol.* **2021**, *426*, 127786. [[CrossRef](#)]

148. Wu, T.; Blawert, C.; Serdechnova, M.; Karlova, P.; Dovzhenko, G.; Florian Wieland, D.C.; Stojadinovic, S.; Vasilic, R.; Mojsilovic, K.; Zheludkevich, M.L. Formation of Plasma Electrolytic Oxidation Coatings on Pure Niobium in Different Electrolytes. *Appl. Surf. Sci.* **2022**, *573*, 151629. [[CrossRef](#)]
149. Hussein, R.O.; Nie, X.; Northwood, D.O. Influence of Process Parameters on Electrolytic Plasma Discharging Behaviour and Aluminum Oxide Coating Microstructure. *Surf. Coatings Technol.* **2010**, *205*, 1659–1667. [[CrossRef](#)]
150. Li, J.; Cai, H.; Jiang, B. Growth Mechanism of Black Ceramic Layers Formed by Microarc Oxidation. *Surf. Coatings Technol.* **2007**, *201*, 8702–8708. [[CrossRef](#)]
151. Kalkanci, H.; Kurnaz, S.C. The Effect of Process Parameters on Mullite-Based Plasma Electrolytic Oxide Coatings. *Surf. Coatings Technol.* **2008**, *203*, 15–22. [[CrossRef](#)]
152. Lu, X.; Mohedano, M.; Blawert, C.; Matykina, E.; Arrabal, R.; Kainer, K.U.; Zheludkevich, M.L. Plasma Electrolytic Oxidation Coatings with Particle Additions—A Review. *Surf. Coatings Technol.* **2016**, *307*, 1165–1182. [[CrossRef](#)]
153. Lu, X.; Blawert, C.; Zheludkevich, M.L.; Kainer, K.U. Insights into Plasma Electrolytic Oxidation Treatment with Particle Addition. *Corros. Sci.* **2015**, *101*, 201–207. [[CrossRef](#)]
154. Lu, X.; Blawert, C.; Huang, Y.; Ovri, H.; Zheludkevich, M.L.; Kainer, K.U. Plasma Electrolytic Oxidation Coatings on Mg Alloy with Addition of SiO₂ Particles. *Electrochim. Acta* **2016**, *187*, 20–33. [[CrossRef](#)]
155. Tu, W.; Zhu, Z.; Zhuang, X.; Cheng, Y.; Skeldon, P. Effect of Frequency on Black Coating Formation on AZ31 Magnesium Alloy by Plasma Electrolytic Oxidation in Aluminate-Tungstate Electrolyte. *Surf. Coat. Technol.* **2019**, *372*, 34–44. [[CrossRef](#)]
156. Tang, M.; Feng, Z.; Li, G.; Zhang, Z.; Zhang, R. High-Corrosion Resistance of the Microarc Oxidation Coatings on Magnesium Alloy Obtained in Potassium Fluotitanate Electrolytes. *Surf. Coatings Technol.* **2015**, *264*, 105–113. [[CrossRef](#)]
157. Sreekanth, D.; Rameshbabu, N.; Venkateswarlu, K. Effect of Various Additives on Morphology and Corrosion Behavior of Ceramic Coatings Developed on AZ31 Magnesium Alloy by Plasma Electrolytic Oxidation. *Ceram. Int.* **2012**, *38*, 4607–4615. [[CrossRef](#)]
158. Song, L.; Kou, Y.; Song, Y.; Shan, D.; Zhu, G.; Han, E.H. Fabrication and Characterization of Micro-Arc Oxidation (MAO) Coatings on Mg-Li Alloy in Alkaline Polyphosphate Electrolytes without and with the Addition of K₂TiF₆. *Mater. Corros.* **2011**, *62*, 1124–1132. [[CrossRef](#)]
159. Sreekanth, D.; Rameshbabu, N.; Venkateswarlu, K.; Subrahmanyam, C.; Rama Krishna, L.; Prasad Rao, K. Effect of K₂TiF₆ and Na₂B₄O₇ as Electrolyte Additives on Pore Morphology and Corrosion Properties of Plasma Electrolytic Oxidation Coatings on ZM21 Magnesium Alloy. *Surf. Coatings Technol.* **2013**, *222*, 31–37. [[CrossRef](#)]
160. Hakimizad, A.; Raeissi, K.; Golozar, M.A.; Lu, X.; Blawert, C.; Zheludkevich, M.L. Influence of Cathodic Duty Cycle on the Properties of Tungsten Containing Al₂O₃/TiO₂ PEO Nano-Composite Coatings. *Surf. Coatings Technol.* **2018**, *340*, 210–221. [[CrossRef](#)]
161. Wang, L.; Zhou, J.; Liang, J.; Chen, J. Thermal Control Coatings on Magnesium Alloys Prepared by Plasma Electrolytic Oxidation. *Appl. Surf. Sci.* **2013**, *280*, 151–155. [[CrossRef](#)]
162. Hakimizad, A.; Raeissi, K.; Santamaria, M.; Asghari, M. Effects of Pulse Current Mode on Plasma Electrolytic Oxidation of 7075 Al in Na₂WO₄ Containing Solution: From Unipolar to Soft-Sparking Regime. *Electrochim. Acta* **2018**, *284*, 618–629. [[CrossRef](#)]
163. Yao, Z.; Hu, B.; Shen, Q.; Niu, A.; Jiang, Z.; Su, P.; Ju, P. Preparation of Black High Absorbance and High Emissivity Thermal Control Coating on Ti Alloy by Plasma Electrolytic Oxidation. *Surf. Coatings Technol.* **2014**, *253*, 166–170. [[CrossRef](#)]
164. Li, K.; Li, W.; Zhang, G.; Guo, P. Preparation of Black PEO Layers on Al-Si Alloy and the Colorizing Analysis. *Vacuum* **2015**, *111*, 131–136. [[CrossRef](#)]
165. Lukiyanchuk, I.V.; Rudnev, V.S.; Tyrina, L.M. Plasma Electrolytic Oxide Layers as Promising Systems for Catalysis. *Surf. Coatings Technol.* **2016**, *307*, 1183–1193. [[CrossRef](#)]
166. Hwang, I.J.; Hwang, D.Y.; Kim, Y.M.; Yoo, B.; Shin, D.H. Formation of Uniform Passive Oxide Layers on High Si Content Al Alloy by Plasma Electrolytic Oxidation. *J. Alloys Compd.* **2010**, *504*, S527–S530. [[CrossRef](#)]
167. Wang, J.M.; Tsai, D.S.; Tsai, J.T.J.; Chou, C.C. Coloring the Aluminum Alloy Surface in Plasma Electrolytic Oxidation with the Green Pigment Colloid. *Surf. Coatings Technol.* **2017**, *321*, 164–170. [[CrossRef](#)]
168. Yeh, S.C.; Tsai, D.S.; Wang, J.M.; Chou, C.C. Coloration of the Aluminum Alloy Surface with Dye Emulsions While Growing a Plasma Electrolytic Oxide Layer. *Surf. Coatings Technol.* **2016**, *287*, 61–66. [[CrossRef](#)]
169. Xue, W.; Shi, X.; Hua, M.; Li, Y. Preparation of Anti-Corrosion Films by Microarc Oxidation on an Al-Si Alloy. *Appl. Surf. Sci.* **2007**, *253*, 6118–6124. [[CrossRef](#)]
170. Krishtal, M.M. Effect of Structure of Aluminum-Silicon Alloys on the Process of Formation and Characteristics of Oxide Layer in Microarc Oxidizing. *Met. Sci. Heat Treat.* **2004**, *46*, 377–384. [[CrossRef](#)]
171. Wang, L.; Nie, X. Silicon Effects on Formation of EPO Oxide Coatings on Aluminum Alloys. *Thin Solid Films* **2006**, *494*, 211–218. [[CrossRef](#)]
172. Feng Su, J.; Nie, X.; Hu, H.; Tjong, J. Friction and Counterface Wear Influenced by Surface Profiles of Plasma Electrolytic Oxidation Coatings on an Aluminum A356 Alloy. *J. Vac. Sci. Technol. A Vacuum Surf. Film.* **2012**, *30*, 061402. [[CrossRef](#)]
173. Moshrefifar, M.; Ebrahimifar, H.; Hakimizad, A. Systematic Investigation of Silicon Content Effects on the PEO Coatings' Properties on Al-Si Binary Alloys in Silicate-Based and Tungstate-Containing Electrolytes. *Coatings* **2022**, *12*, 1438. [[CrossRef](#)]
174. Student, M.; Pohrelyuk, I.; Padgurskas, J.; Posuvailo, V.; Hvozdet's'kyi, V.; Zadorozhna, K.; Chumalo, H.; Veselivska, H.; Kovalchuk, I.; Kychma, A. Influence of Plasma Electrolytic Oxidation of Cast Al-Si Alloys on Their Phase Composition and Abrasive Wear Resistance. *Coatings* **2023**, *13*, 637. [[CrossRef](#)]

175. Mora-Sanchez, H.; del Olmo, R.; Rams, J.; Torres, B.; Mohedano, M.; Matykina, E.; Arrabal, R. Hard Anodizing and Plasma Electrolytic Oxidation of an Additively Manufactured Al-Si Alloy. *Surf. Coatings Technol.* **2021**, *420*, 127339. [[CrossRef](#)]
176. Pezzato, L.; Dabalà, M.; Brunelli, K. Microstructure and Corrosion Properties of PEO Coatings Produced on Am-Aluminum Alloys. *Key Eng. Mater.* **2019**, *813*, 298–303. [[CrossRef](#)]
177. Pezzato, L.; Dabalà, M.; Gross, S.; Brunelli, K. Effect of Microstructure and Porosity of AlSi10Mg Alloy Produced by Selective Laser Melting on the Corrosion Properties of Plasma Electrolytic Oxidation Coatings. *Surf. Coatings Technol.* **2020**, *404*, 126477. [[CrossRef](#)]
178. Li, K.; Li, W.; Zhang, G.; Wang, M.; Tang, P. Influence of Surface Etching Pretreatment on PEO Process of Eutectic Al-Si Alloy. *Chin. J. Chem. Eng.* **2015**, *23*, 1572–1578. [[CrossRef](#)]
179. Li, K.; Li, W.; Yi, A.; Zhu, W.; Liao, Z.; Chen, K.; Li, W. Tuning the Surface Characteristic of Al-Si Alloys and Its Impacts on the Formation of Micro Arc Oxidation Layers. *Coatings* **2021**, *11*, 453. [[CrossRef](#)]
180. Li, K.; Li, W.; Zhang, G.; Zhu, W.; Zheng, F.; Zhang, D.; Wang, M. Effects of Si Phase Refinement on the Plasma Electrolytic Oxidation of Eutectic Al-Si Alloy. *J. Alloys Compd.* **2019**, *790*, 650–656. [[CrossRef](#)]
181. Hu, C.J.; Hsieh, M.H. Preparation of Ceramic Coatings on an Al-Si Alloy by the Incorporation of ZrO₂ Particles in Microarc Oxidation. *Surf. Coatings Technol.* **2014**, *258*, 275–283. [[CrossRef](#)]
182. Polunin, A.V.; Cheretaeva, A.O.; Borgardt, E.D.; Rastegaev, I.A.; Krishtal, M.M.; Katsman, A.V.; Yasnikov, I.S. Improvement of Oxide Layers Formed by Plasma Electrolytic Oxidation on Cast Al-Si Alloy by Incorporating TiC Nanoparticles. *Surf. Coatings Technol.* **2021**, *423*, 127603. [[CrossRef](#)]
183. Krishtal, M.M.; Katsman, A.V.; Polunin, A.V. Effects of Silica Nanoparticles Addition on Formation of Oxide Layers on Al[Si] Alloy by Plasma Electrolytic Oxidation: The Origin of Stishovite under Ambient Conditions. *Surf. Coatings Technol.* **2022**, *441*, 128556. [[CrossRef](#)]

Disclaimer/Publisher’s Note: The statements, opinions and data contained in all publications are solely those of the individual author(s) and contributor(s) and not of MDPI and/or the editor(s). MDPI and/or the editor(s) disclaim responsibility for any injury to people or property resulting from any ideas, methods, instructions or products referred to in the content.